OF 2007-4

New Nouveau
Brunswick

Open File

Natural Resources
Minerals, Policy and Planning

REFLECTION SEISMIC DATA PROCESSING OF THE HEATH STEELE 2D SIDE-SWIPE SURVEY

Brian Roberts, Erick Adam, Suzanne Woelz
Geological Survey of Canada

For:

Noranda Mining and Exploration,
Atlantic Canada Region

ISSN 1702-2649
ISBN 978-1-55396-392-9
Price: $7.00

2007

Open File 2007-4

Reflection Seismic Data Processing of the Heath
Steele 2D Side-swipe Survey

Recommended citation:

Roberts, B., Adam, E., and Woelz, S. 2007. Reflection Seismic Data Processing of the Heath Steele 2D Side-swipe Survey (1999). New Brunswick Department of Natural Resources; Minerals, Policy and Planning Division, Open File Report 2007-4, 37 p.

Prepared for:

Minerals, Policy and Planning Division
Department of Natural Resources
Province of New Brunswick

Hon. Donald Arsenault
Minister of Natural Resources

March 2007

New Nouveau
Brunswick

Natural Resources
Minerals, Policy and Planning

Open File 2007-4

REFLECTION SEISMIC DATA PROCESSING OF THE HEATH STEELE 2D SIDE-SWIPE SURVEY

Brian Roberts, Erick Adam, Suzanne Woelz
Geological Survey of Canada

For:

Noranda Mining and Exploration,
Atlantic Canada Region

This report has been prepared by the Geological Survey of Canada for the Province of New Brunswick. The document has been published as received from the author.

Value-added/Mineral Processing Program report received October, 1999

Le présent rapport a été préparé par la Commission géologique du Canada d'Ottawa, Ontario, à l'intention de la province du Nouveau-Brunswick. Le document a été publié sous la forme où il a été reçu de l'auteur.

Rapport du Programme de traitement des minéraux à valeur ajoutée reçu en octobre 1999.

ISSN 1702-2649
ISBN 978-1-55396-392-9
Price: $7.00

2007

REPORT

Reflection Seismic Data Processing of the Heath Steele 2D Side-swipe Survey

BY

Brian Roberts, Erick Adam, Suzanne Woelz

Geological Survey of Canada
Continental Geoscience Division
Ottawa, Ontario

FOR

Noranda Mining and Exploration
Atlantic Canada Region

As fulfillment of an SPA between Noranda and the GSC initiated in July 1999

October, 1999

Introduction

In 1998 Noranda Mining and Exploration collected a 2D side-swipe survey in the vicinity of the Heath Steele mining camp in New Brunswick (Petrie and Woods, 1999). The objective of the experiment was to examine the possibility of using 2D seismic techniques to image reflected/scattered energy from vertically dipping stratigraphy. The main Heath horizon represents about 5 km of prospective stratigraphy with known sulphide deposits. It has been previously documented that Noranda's Bathurst mining camp is a favorable setting for using seismic techniques to delineate mineralized zones in an otherwise complicated stratigraphic setting (Salisbury et al., 1997). The host rocks generally have very little impedance contrast with each other, however the ore zones can produce a large contrast depending on the amount of pyrite and calcopyrite present. This experiment involved the acquisition of high resolution 2D seismic data which was positioned along strike and offset from the main mine horizon, hence the name "side-swipe"

The initial processing failed to image the target horizon and no reflections were observed in the top 0.4 s. Thus, the objective of this study is to enhance the shallow reflections and then identify anomalous scattering responses, possibly associated with mineralization.

Data Acquisition

The data acquisition parameters are summarized in Table 1. It was realized from the start that optimal shot and receiver coupling would be required to achieve the necessary signal to noise levels. Shot holes were drilled to a depth of 6 m and preloaded with dynamite. The loose ground cover was removed at each receiver station to enable good geophone plants.

Table 1. Acquisition Parameters

Line length:	6.32 km
RX interval:	10 m
SP interval:	40 m (20 m on east end)
Number of SP:	227
Charge size:	.5 kg Dynoseis
Sampling Rate:	2 ms
Record length:	3 s

Processing

The data processing sequence and parameters are summarized in Table 2. The prestack processing of the shot gathers focuses mainly on the elimination of noise, including source generated, ambient background and mine related noise, the application of static corrections, and the determination of the correct velocity function for stacking the data (including the application of dip moveout correction). Noise elimination is critical because in the crystalline environment we are dealing with low reflection coefficients and thus, a low signal-to-noise ratio. The processing has been performed with the ProMAX seismic data processing package with some specific steps done with the INSIGHT (spectral balancing) and GLI3D (refraction statics) software packages.

Table 2. Processing Sequence

1) Geometry
2) Frequency filter; 10.5, 12.8, 14.8, 18.1, 19.6, 21.4, 27.0, 29.6, 32.4, 60.0, 69.6, 74.7, 94.9 Hz (HARMON)
3) First break picking and trace edits
4) Gain application; 500 ms AGC
5) Bandpass filter; 30-120 Hz
6) Front mute
7) Brute stack
8) Refraction statics (GLI3D)
9) Spectral Balancing; 30-120 Hz in 10 Hz bands
10) Dip Moveout correction
11) Velocity analysis; every 50 CDP's
12) NMO correction and stack; 70% stretch mute and alpha trimmed mean stack
13) Bandpass filter
14) Kirchhoff depth migration
15) Gain application; 500 ms AGC

Below we have listed the highlights of the processing sequence with applicable comments.

1) Geometry definition

The seismic line was quite straight with one bend (Figure 1), so a straight CDP processing line could be fitted through the data. The CDP fold is as high as 231 in the middle of the line, smoothly tapering to a low fold at the ends of the line. Elevations vary by close to 100 m along the length of the line.

2) Removal of electrical noise

By examining the raw shot gathers we identified the basic types of noise which need to be dealt with; 1) coherent source generated noise (ground roll and shear wave) 2) coherent noise related to nearby mining activity and 3) electrical noise from local infrastructure (Figure 2). The coherent source generated noise will be addressed later and the mine noise should be discriminated from the useful signal during the NMO/stacking process. The electrical noise is of sufficient amplitude that we want to remove it prior to first break picking and do so without affecting nearby frequencies. We used a program called HARMON (Adam and Langlois, 1995) to eliminate this monofrequency noise from the data. From the spectral analysis of a number of shotpoints it was determined that the following frequencies should be removed (Figures 3a and 3b):

10.5, 12.8, 14.8, 18.1, 19.6, 21.4, 27.0, 29.6, 32.4, 60.0, 69.6, 74.7, 94.9 Hz

HARMON will search a small window around each target frequency for the exact frequency of the noise and eliminate it.

3) First break picking / trace editing

The first breaks were picked using a neural network picker in ProMAX and then cleaned up by inspecting each shot gather. The only trace editing required involved killing two shot records (FFID 67 and 231).

4) Gain application

Since we are attempting to enhance any reflectivity in these data and not necessarily preserve relative amplitudes a 500 ms automatic gain control (AGC) was applied at this point.

5) Bandpass filter

The low frequency end of the spectrum is primarily dominated by dispersive ground roll energy and air blast along with ambient noise related to workings at the mine site, small streams, etc. To remove this energy the low cut of the bandpass filter was set at 30 Hz. The shot gathers also contain abundant high frequency energy, beyond 200 Hz, but the frequency analysis revealed that the reflective energy in the shot gathers was below 120 Hz. The bandpass filter was thus set to be quite wide, between 30-120 Hz, at this early stage of the processing.

6) Trace muting

A top mute defined by the first break picks was applied to all the shot gathers. The data is muted to 30 ms after the first breaks, tapering to no mute at 50 ms after the first breaks.

7) Brute stack

A brute stack was done using a simple velocity function and we observed some strong reflectivity both at depth and near surface.

8) Refraction statics application

This static correction is vital in obtaining a good seismic image in any mining camp scale seismic survey.

Delays in first break arrival times are caused by the low velocity sediments and altered rock formation in the near surface. It is necessary to compensate for these delays to ensure that the high frequencies of the data survive the stacking process. GLI3D program from Hampson-Russell was used to derive the near surface model (velocity and thickness) from the complete database of first break pick times (143,691 in total). Given our previous experience with this software in other mining camps (Matagami and Manitouwadge), we did not try other refraction static correction methods. However, the commercial stack used the Green Mountain Geophysical package.

Two algorithms are available to compute static corrections in GLI3D and they were both tested. One method performs a tomographic inversion of the first break picks while the other is the standard generalized linear inversion (Hampson and Russell, 1984). The static corrections obtained using the two methods were similar and the main difference was in the execution time (the tomographic inversion is quite slow). We also computed the refraction static correction using a limited range of offsets (0-1 km). When only data from shot-receiver distances of less than 1 km were used, the average first break error was reduced to 1.87 ms, from 4.48 ms when all data was used. The final stack section generated using static corrections derived from the limited offset database was not as good as the one obtained from all the first break pick times. Thus, the static solution used to stack the Heath Steele seismic data was generated with the following parameters:

Total picks: 143,691
Picks rejected after 1 iteration with an error > 13 ms: 4 018
Number of geological model iterations: 3
Number of conjugate model iteration: 20
Number of layers: 1
Velocity of the first layer: 1000 m/s (fixed)
Replacement velocity: 5400 m/s
Datum: 400 m ASL
Uphole time data could not be used (generated NaN in GLI3D)
GLI3D version: 4.0

The final combined static solution and datum corrections revealed that shot statics were as high as 16 ms and the receiver statics were as high as 18 ms. Consequently, the maximum total static correction is 34 ms. The importance of these static corrections can be estimated if we consider the period of a 100 Hz signal: 10 ms or 54 m (at 5400 m/s). On the Heath Steel seismic line the amplitude of the maximum static correction is 3 times the period of a 100 Hz signal. The effect of not correcting for near surface variations is a low frequency stack section and poor resolution.

The source and receiver statics used to correct for the weathering layer are shown in Figure 4. A noticeable improvement was noted in the stack section after applying the refraction statics, but it was mostly an enhanced coherency in the major reflectors already identified in the brute stack.

9) Spectral Balancing

We tested both FK filtering and 2D spatial filtering as ways of filtering out the coherent source generated noise in the shot gathers. Both techniques are effective, but we felt they also somewhat affected the reflected energy. Since a good portion of the ground roll and shear wave energy is in the lower end of the frequency spectrum, whitening the spectrum has the effect of lowering the amplitude of these signals. Spectral balancing is very effective with data that has a wide spectrum like the Heath Steele line. We applied spectral balancing from 30 – 120 Hz in 10 Hz bands.

Figure 5 displays the shot gather from Figure 2 at this stage in the processing.

At this point in the processing we break into two flows, one for pre-stack migration and one for dip moveout correction (DMO) and post-stack migration. These two flows should produce complimentary sections and the superior image can be used for interpretation. The pre-stack migration technique will be discussed separately following the description of the processing steps.

10) Dip moveout correction (DMO)

As in many complex geological environments, we observe both dipping and subhorizontal reflections along the Heath Steele line. The dipping events are typically related to steeply dipping contacts/faults, or diffractions from structural discontinuities and high impedance scatterers. In applying the normal moveout correction there is no velocity function that will simultaneously optimize stacking of both dipping and sub-horizontal events. The dipping events stack at anomalously high velocities. To circumvent this problem, DMO is used to effectively create a zero-offset section, in which dipping events will stack at realistic velocities. Prior to DMO a first-pass velocity function is used to correct the data, then a full velocity analysis is performed following DMO.

11) Velocity Analysis

The velocity analysis was performed using a combined semblance/constant velocity stack display every 50 CDP's (250 m). The picked velocity function was then used to rerun DMO and then a final velocity function was selected .

12) Normal moveout (NMO) correction and CDP stack

Following some tests of the NMO stretch mute, a NMO correction was applied to the data and an alpha-trimmed mean stack with a maximum fold of 231 was performed. Any data stretched by more than 70% was muted.

Poststack

13) Bandpass filter

Up to this point we have maintained a wide frequency spectrum in the data. This is to ensure that every chance is given to enhance the high frequency data, especially in the top .5 s. In analyzing the data poststack it is observed that most of the coherent energy lies in the 30-80 Hz range, but there is also some higher frequency signal (up to 120 Hz) in the upper part of the section. Because of this, the same bandpass filter that was applied earlier in step 5) was reapplied to remove any spurious noise added during the previous steps.

14) Kirchhoff Depth Migration

A Kirchhoff depth migration was performed using the maximum possible aperture and a maximum dip of 45 degrees. Frequencies up to 120 Hz were migrated.

15) Automatic Gain Control (AGC)

A scale factor is calculated using a 500 ms window and applied to the sample at the centre of the window.

Figure 6 displays the final DMO structure stack and figure 7 displays the migrated stack. Larger versions of these stack sections are provided as folded inserts.

Equivalent Offset Migration

Equivalent offset prestack migration (EOM) has been applied to the Heath Steele side-swipe line using an ITA/Insight module developed at the GSC. The theory and potential applications of equivalent offset migration are described by Bancroft et al. (1998). For a constant velocity the typical NMO, DMO, CMP stack process is kinematically equivalent to prestack migration (Hale, 1984). However, EOM provides an efficient method for acquiring detailed velocity information and comparisons with poststack migrations have shown that equivalent offset migrations have better coherency and hence, are more interpretable (Bancroft, 1998). In the application of this method common scatter point (CSP) gathers are assembled at the CDP locations along the processing line.

A CSP bin width of 20 m was selected based on receiver spacing and trial-and-error testing with other data, and a CSP gather was generated at each CDP location. Each CSP gather consisted of 500 traces with equivalent offsets between 0 and 10,000 m. Note that different bin sizes were not tested. The migration velocity used to assemble the CSP gathers was 5.4 km/s and the maximum migration time is 3 s. The 3 s maximum migration time and the large offsets (10 km) were selected to avoid excessive smearing at depth.

The input traces for the CSP migration have been pre-processed using the pre-stack processing flow described above up to and including the spectral balancing step. After the CSP gathers were assembled, NMO corrections and stacking were performed using ITA/Insight software. A velocity function was selected by doing semblance analysis and stacks were made with this function and an single velocity function which represented an average (.2 s – 5100 m/s, .4 s - 5300 m/s, .6 s – 5500 m/s, .75 – 5700 m/s). The stacks were very similar, but some events were preferentially highlighted on one or the other section. It was decided that the stack using the single velocity function gave the best overall image. There was no NMO stretch mute applied, but a bandpass filter from 40 – 120 Hz was used to remove the low frequency part of the stretched signal. The final processing applied to the EOM section was a mild coherency filter using an ITA/Insight module called smb_smooth. This was performed in order to reduce the steeply dipping and random noise in the very top part of the section. Figure 8 displays the final EOM stack.

Observations

In this project we have little geological information on which to base a detailed interpretation of the data, however there are some features in the data which we can describe. Firstly, we do note some strong reflectivity in the top .4 s, especially in the east end of the profile, and this reflectivity can be followed across the section as it gently dips from .2 s in the east to .75 s at the west end of the line. This dipping package is crossed by some weaker subhorizontal reflectors between .3 and .6 s. At depth we note very strong reflectivity at .9, 1.2 and 1.6 s. These reflections are west dipping on the DMO stack, but after migration we note that they flatten out towards the west and become more or less subhorizontal.

We could not identify any obvious diffractions in the top part of the section on the DMO stack. If some exist they are either too weak to identify or are masked by the strong reflectivity in the areas of interest. It is possible that in this case the wavelength of the seismic signal is small compared to the scattering region, thus we would only expect scattering at areas with strong curvature. However, there are some high amplitude anomalies on the EOM and depth migrated sections which may be associated with high impedance contrasts in the vertical Heath Steele stratigraphy. On the EOM stack we see high amplitude reflections between CDP 200 and 400 at about .2 s (~600m) and also near CDP's 801, 1001 and 1101 in the .15 - .2 s range. Some of these events also correlate with scattering anomalies (see the Scattering Analysis section).

Scattering Analysis

Physical rock property and forward modeling studies indicate that high impedance bodies, such as massive sulphides, can be recognized by their characteristic scattering response (Milkereit et al., 1996). While conventional CMP processing can provide high quality 2-D images of the gross structure in an area, the scattering response of offline, commonly dipping bodies is often attenuated. It is necessary to separate the scattering response from the reflection response.

For this project we have approached the scattering analysis with three methods:

1) EOM prestack migration as described above. The scattering response will appear as small, higher amplitude anomalies on the seismic section (Figure 8). These will be difficult to identify as scatterers, but they can be verified with the next two methods.

2) The MUSIC (Multiple Source Imaging Capabilities) algorithm developed at the GSC.

3) A modified prestack Kirchhoff migration algorithm developed by Christof Mueller, Kiel University (Mueller, 1999)

MUSIC

The MUSIC technique is designed to enhance the scattering response at the expense of the reflection response. The method treats local high impedance anomalies as stationary secondary seismic sources in the subsurface. During a seismic experiment each subsurface point is illuminated from many different directions. For each subsurface point, the contributions from multiple source points are stacked to construct the complete scattering image. In the process, all reflected and refracted compressional and shear waves events are effectively attenuated. The scattered energy should show up as a hyperbola with an apex at the closest station number on the 2D line and be focussed best on the MUSIC stack at that station. We ran the MUSIC stack program for depths of 250, 500, 750, 1000, 1500, and 2000 m with appropriate background velocities and by systematically scanning through the "gathers" were able to identify numerous scattering events. Figure 9 displays the EOM migration with the locations of the MUSIC scatterers indicated and examples of the MUSIC stacks for each noted scatterer can be found in Appendix A. These scatterers represent the highest amplitude events identified at the various offsets while scanning through all the MUSIC stacks. Other weaker events are likely present, but would require a more detailed analysis.

Modified Prestack Kirchhoff Migration

In this method a modified prestack Kirchhoff migration is applied to image the position of possible subsurface scatterers. This algorithm is not able to distinguish between the response from a reflecting plane and a point scatterer, but it has the benefit of producing images of scattering centres even when the scattering energy is at noise level. Also, since we are working with a 2D dataset, there will be some ambiguity in the location of a scatterer with respect to the seismic line (as with the MUSIC results). A scatterer at a given distance from the line could fall anywhere on a semi-circular path with an axis defined by the line. If there is already geological information on where scatterers could be expected then this ambiguity can be reduced. At this point we are still experimenting with the best way to use this method in analyzing and visualizing scatterers and the algorithm is still considered to be in the development stage. The results shown here do not represent a full analysis, but offer some examples of what sort of imaging can be achieved.

Show in this report are the results for one East-West line through the area of interest (Figure 10) and three North-South lines at locations where high amplitudes were observed on the East-West line (Figure 11). The location of the scattering analysis lines relative to the seismic line is shown in Figure 1. By far, the highest amplitudes are associated with a broad package of scatterers/reflectors positioned roughly 800 m away from CDP 360/stn 285. There are also prominent anomalies near CDP 490/stn 345 (750 m) and CDP 850/stn 526 (750 m), and a smaller, but high amplitude anomalies at CDP 615/stn 408 (1150 m) and CDP 670/stn 438 (350, 500, 800 m).

Conclusions

The data acquisition of line hst98-001 was superb. Source and receiver coupling appears to have been excellent and the recording parameters were all very well suited to acquiring a high quality, high resolution seismic line.

After completing the processing of this dataset we were provided with the results from the commercial processing of line hst98-001, which is documented in the Noranda report

(Petrie and Woods, 1999), and it is very clear that we have significantly improved the final section. We observe some strong reflectivity in the top .5 s and there is much detail, which can hopefully be interpreted in the context of the known geology for this area. There is no single factor that we can point to for the improved section, in fact we found that our brute stack, with virtually no parameter testing and a single velocity function yielded a better image than the commercial section. Further processing steps, i.e. refraction statics, spectral balancing, velocity analysis, DMO, etc., all improved the image, but only incrementally from the brute stack. With no special processing applied we can only assume that our approach of ensuring that the reflection signal is not deteriorated in the shot gather domain and carefully monitoring what each processing step actually does to the data has lead to the improved section. One of the conclusions of the Noranda report was that the ambient and mine noise levels were too high and had adversely affected the stack. We feel that the observed noise had very little impact on the quality of the seismic data. The ambient noise is generally low frequency (< 30 Hz) or a distinct frequency (e.g. 60 Hz) which can be effectively filtered and the coherent mine noise is effectively removed by the NMO and stacking process.

We have identified a number of anomalies in our scattering analysis, some of which may merit further investigation. The modified Kirchhoff prestack migration technique looks particularly promising and with some improvements in the algorithm and the way we visualize the results it could be a powerful tool in mining camp studies. Also, modelling recently performed at the GSC indicate that by incorporating a relatively small amount of 3D information you can start to focus the scattered energy such that both depth and direction could be determined for a scatterer. By adding some offline shots at regular intervals to a high resolution 2D seismic line, much of the ambiguity could be removed about the actual location of a scatterer.

References

Adam, E., and Langlois, P. 1995. Elimination of monofrequency noise from seismic records. Lithoprobe Seismic Processing Facility Newsletter, v. 8, no. 1, p. 59-65.

Bancroft, J. 1998. The equivalent offset method of prestack time migration. Geophysics, v. 63, no 6, p. 2042-2053.

Hampson, D., and Russell, B. 1984. First-break interpretation using generalized linear inversion. Journal of the Canadian Society of Exploration Geophysicists 20:40-54.

Milkereit, B., Eaton, D., Wu, J. Perron, G., Salisbury, M., Berrer, E., and Morrison, G. 1996. Seismic imaging of massive sulphide deposits, part 2: reflection seismic profiling. Economic Geology, V. 91, p. 829-834.

Mueller, C., and Perron, G. 1999. Imaging Capabilities of Prestack Kirchhoff Migration algorithm for DSI Acquisition Geometries. Unpublished report for DSI Consortium, Geological Survey of Canada, 13 pp.

Petrie, L., and Woods, G. 1999. Seismic Methods in Mineral Exploration, Heath Steele Mines, NB. Unpublished report for the New Brunswick Department of Natural Resources and Energy.

Salisbury, M.H., Milkereit, B., Ascough, G.L., Adair, R., Schmitt, D., and Matthews, L. 1997. Physical properties and seismic imaging of massive sulphides. *In* Proceedings of Exploration 97: Fourth Decennial International Conference on Mineral Exploration, *edited by* A.G. Gubbins, p. 383-390.

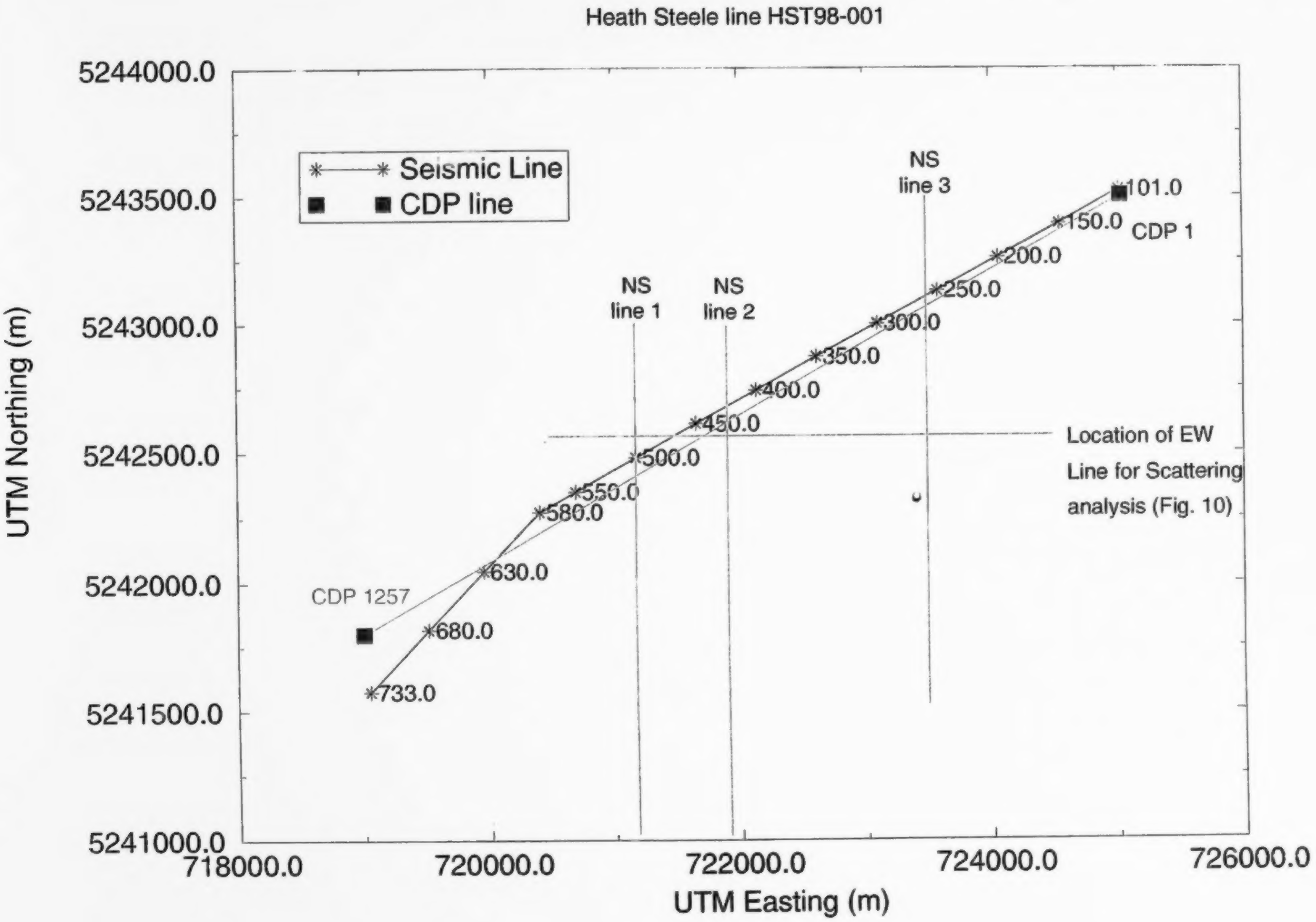

Figure 1. Location map for line HST98-001 and lines used for scattering analysis (UTM zone 19, NAD83).

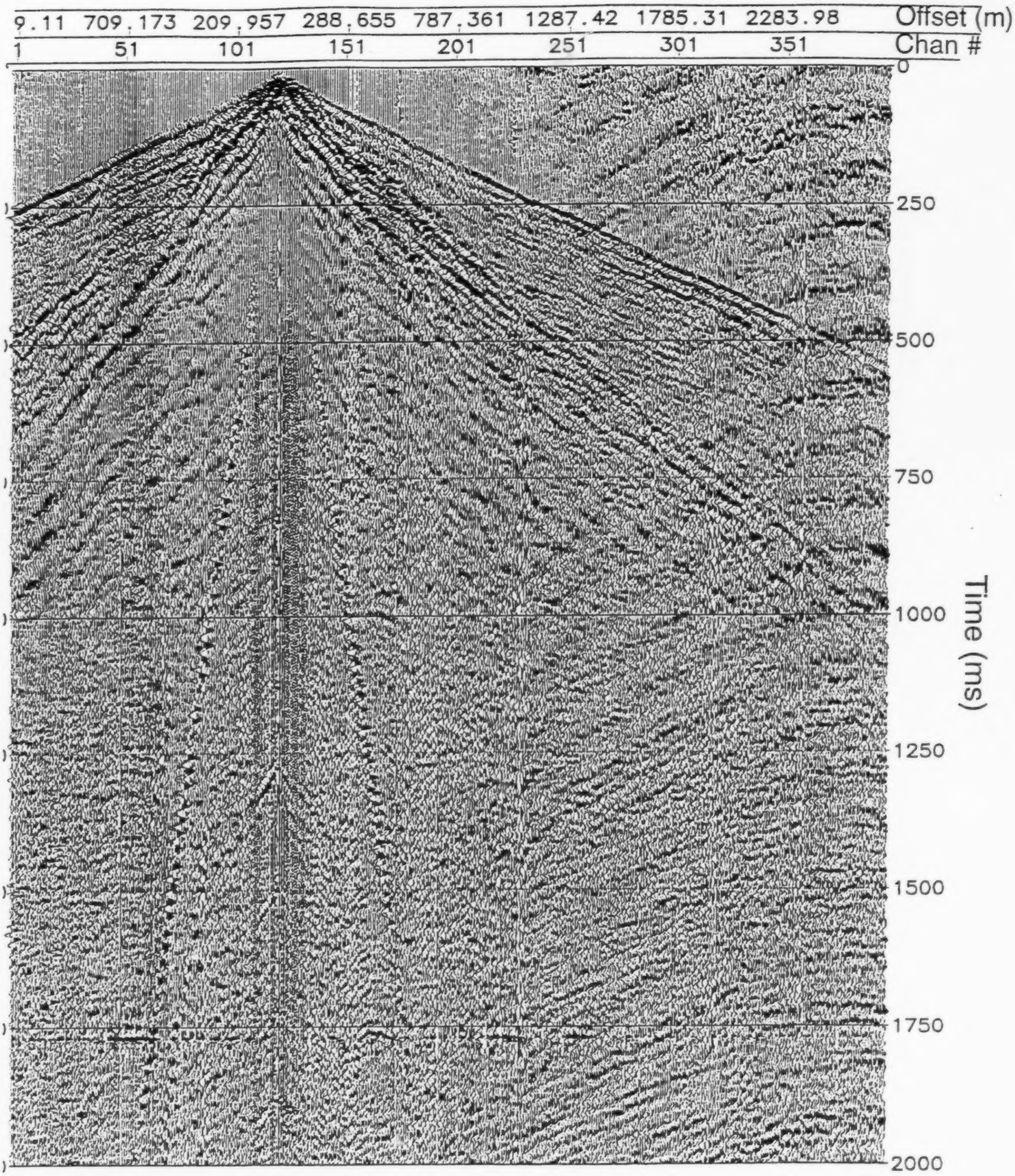

Figure 2. Raw shot gather (ffid 171) from line HST98-001

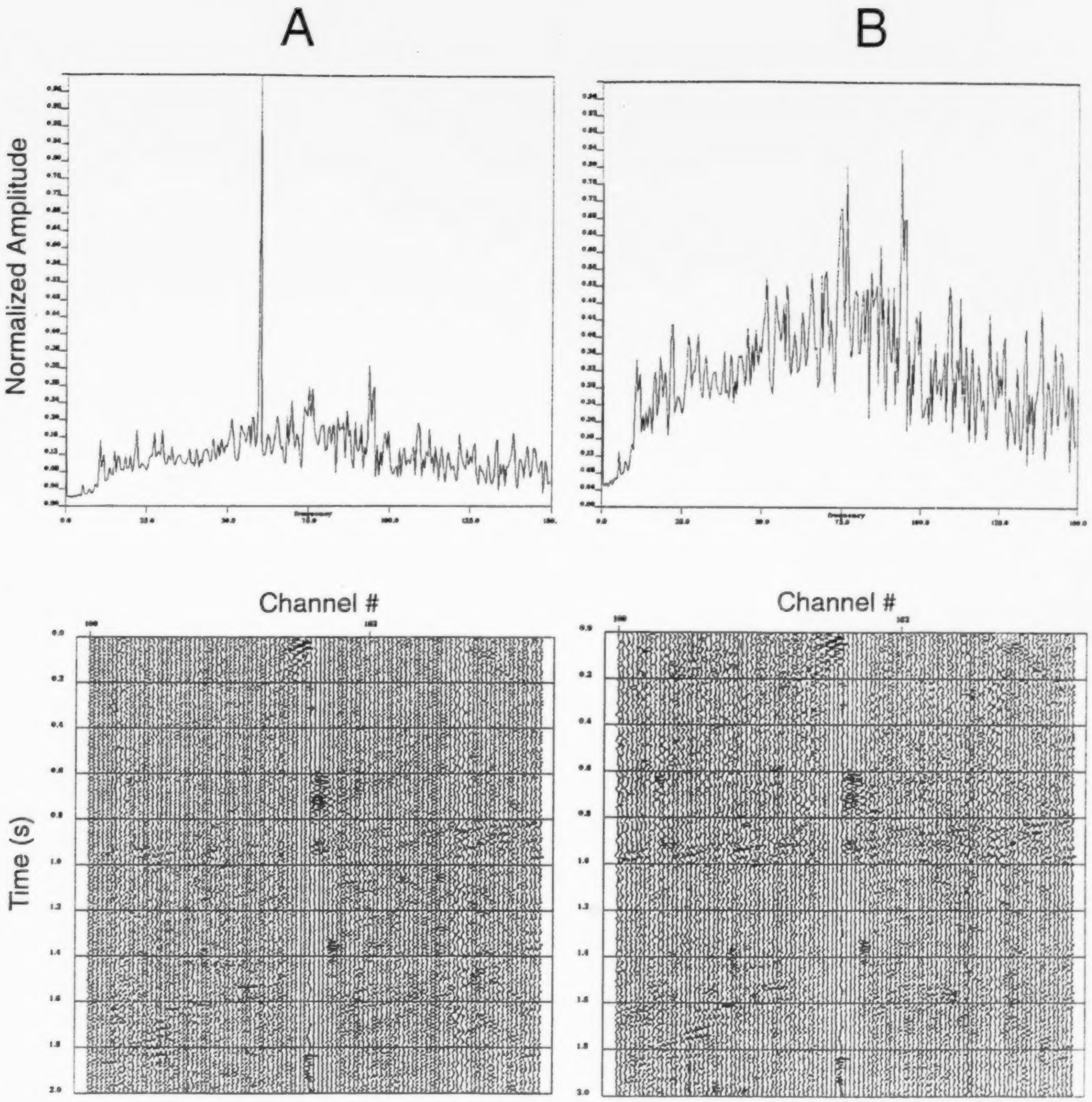

Figure 3a. Frequency spectrum and sample of data (FFID 148) before (A) and after (B) the application of HARMON to reduce monofrequency noise (INSIGHT).

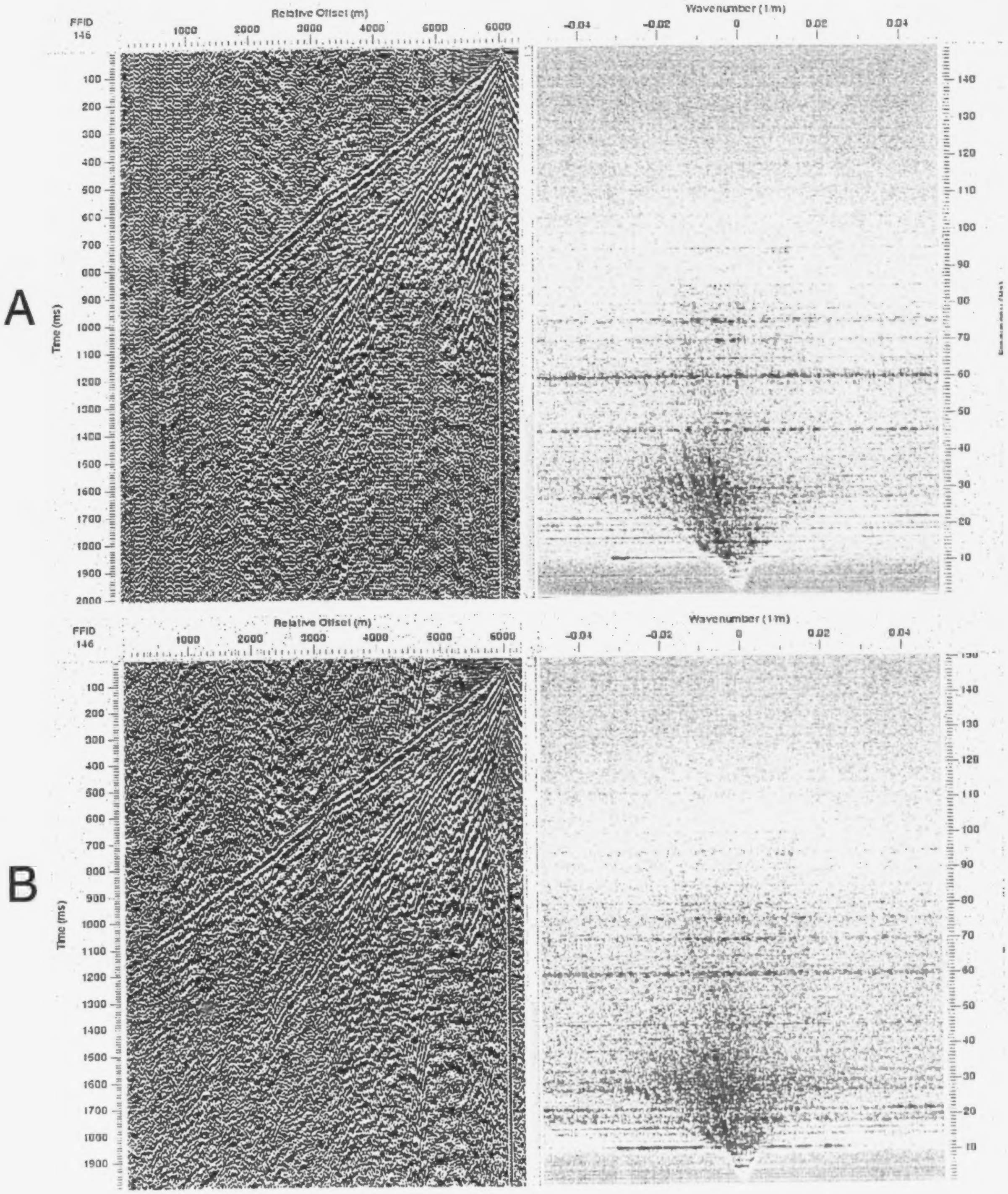

Figure 3b. FK spectrum of FFID 148 before (A) and after (B) the application of HARMON to reduce monofrequency noise (ProMAX). Monofrequency noise appears as flat lines in the FK domain. After removal (B) the noise is still present but greatl attenuated

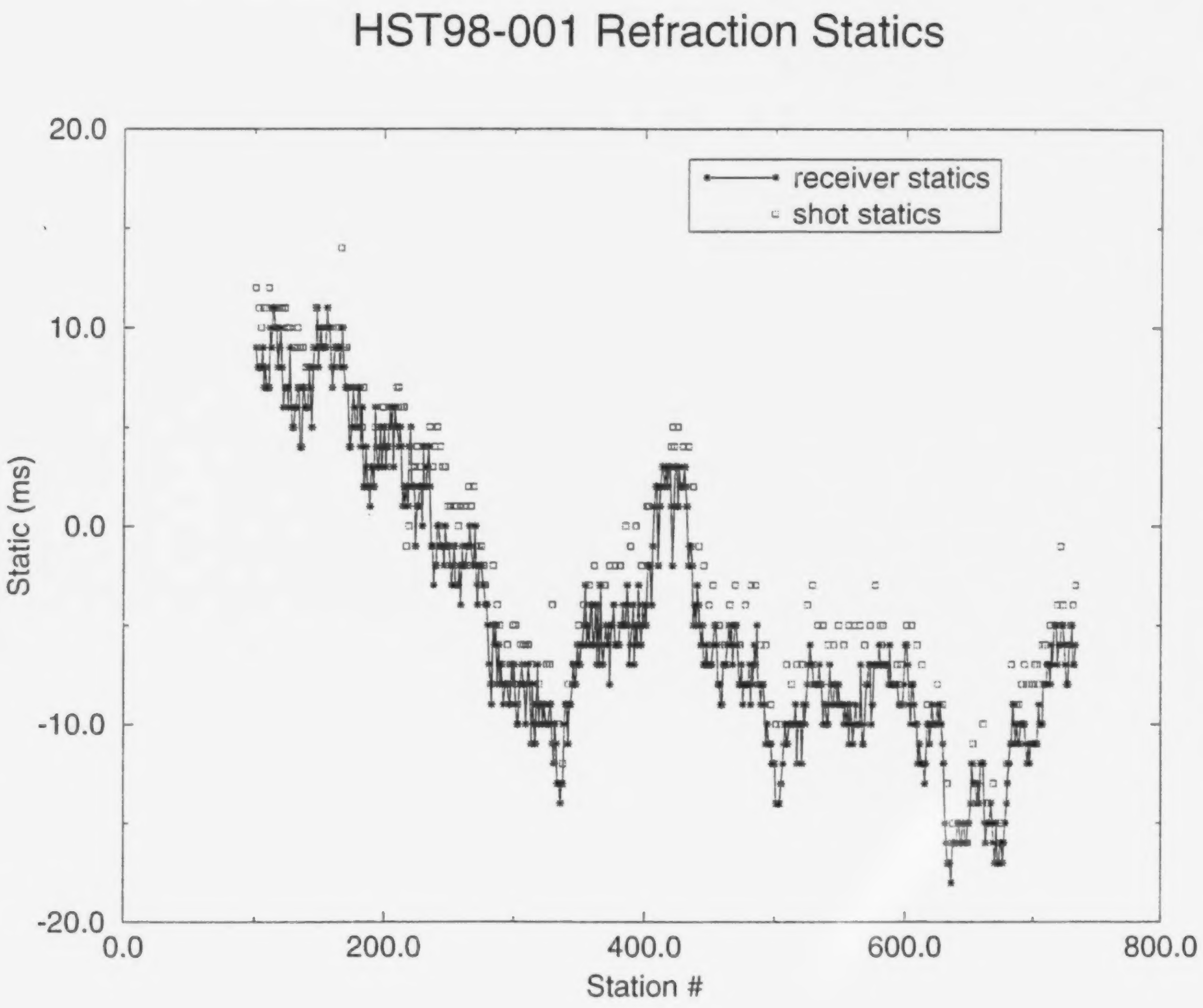

Figure 4. Refraction statics solution (shot and receiver) from GLI3D that was applied to line HST98-001

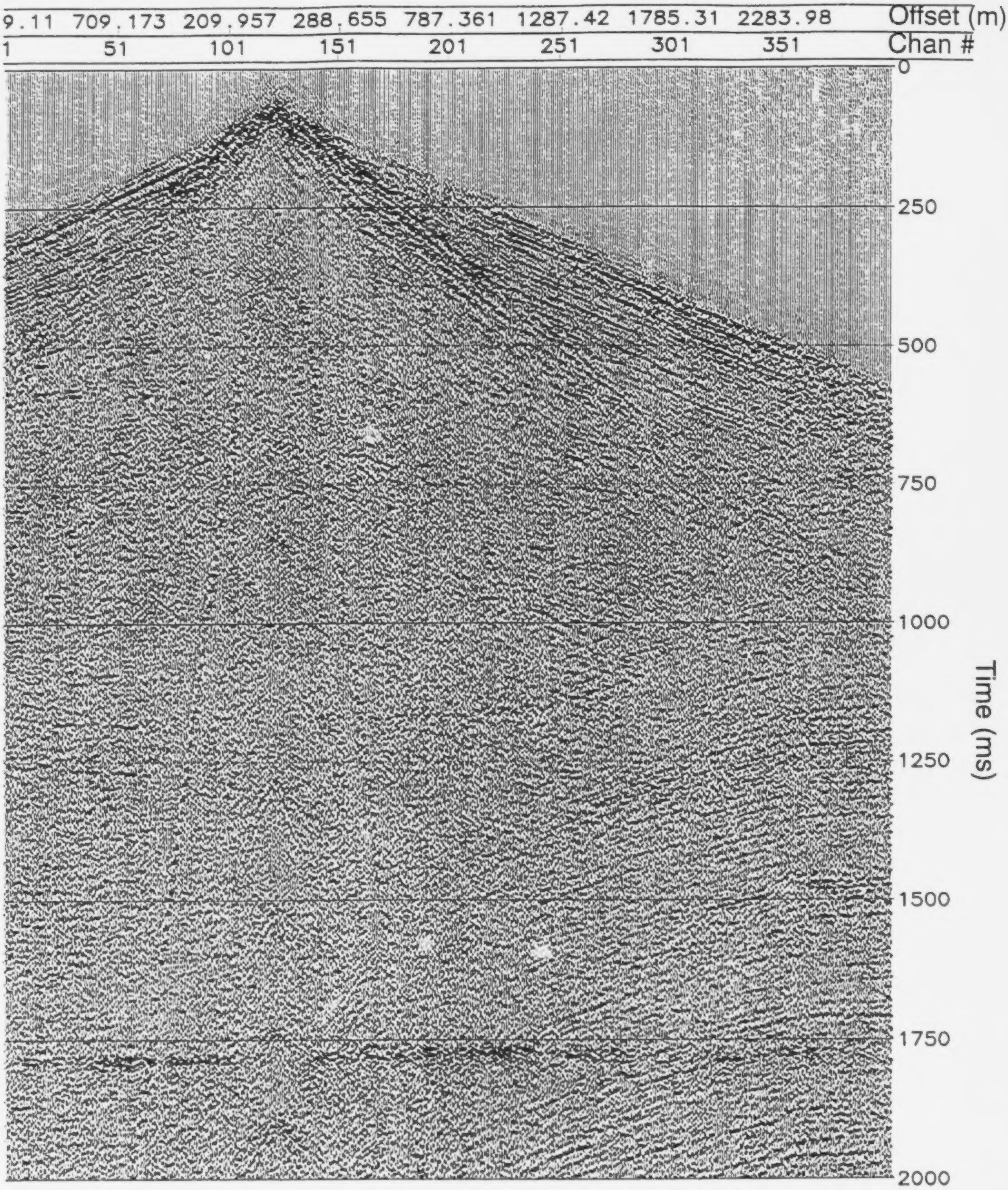

Figure 5. Processed shot gather (ffid 171, 400 traces). This can be compared with Figure 2

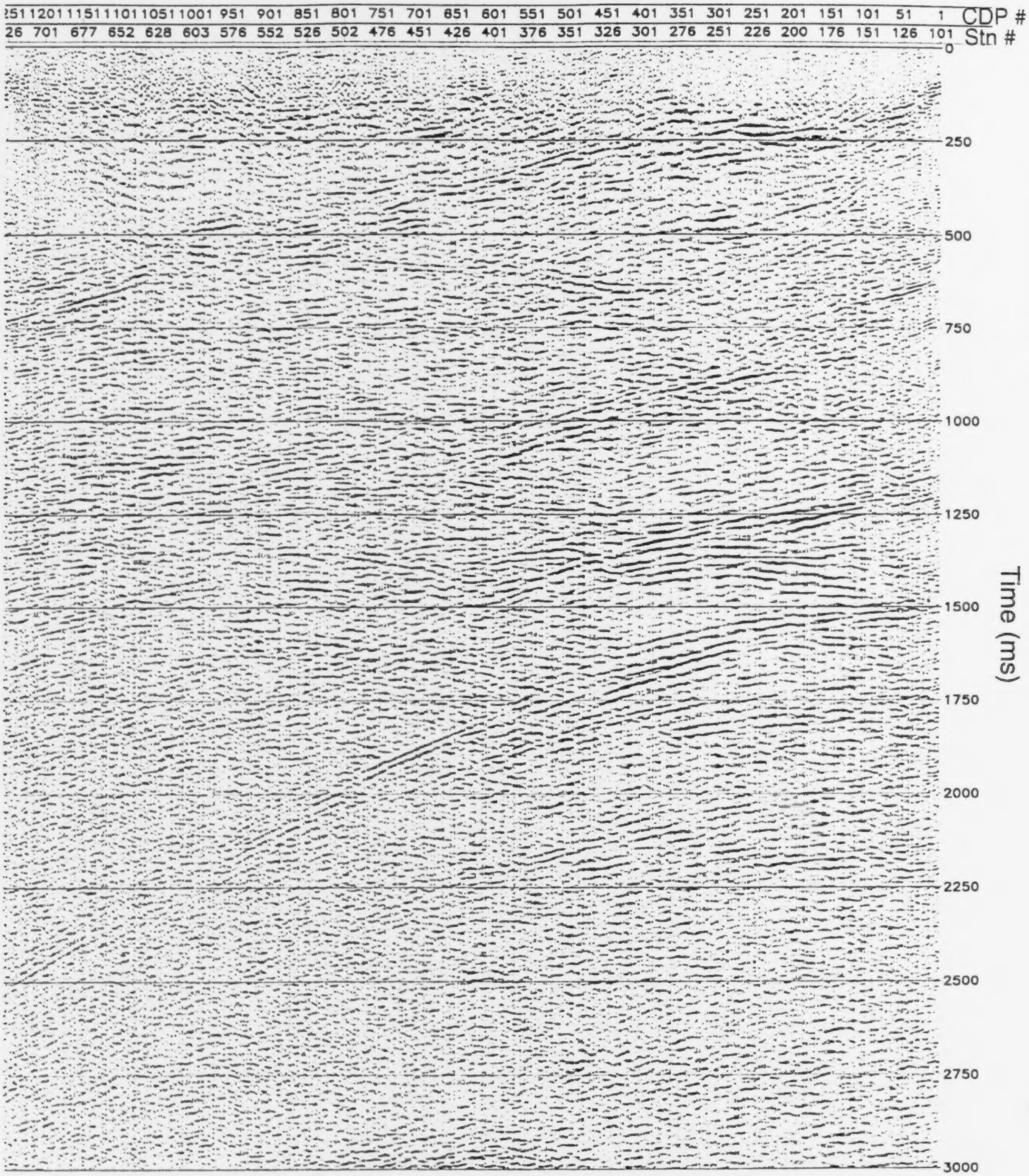

Figure 6. DMO stack line HST98-001

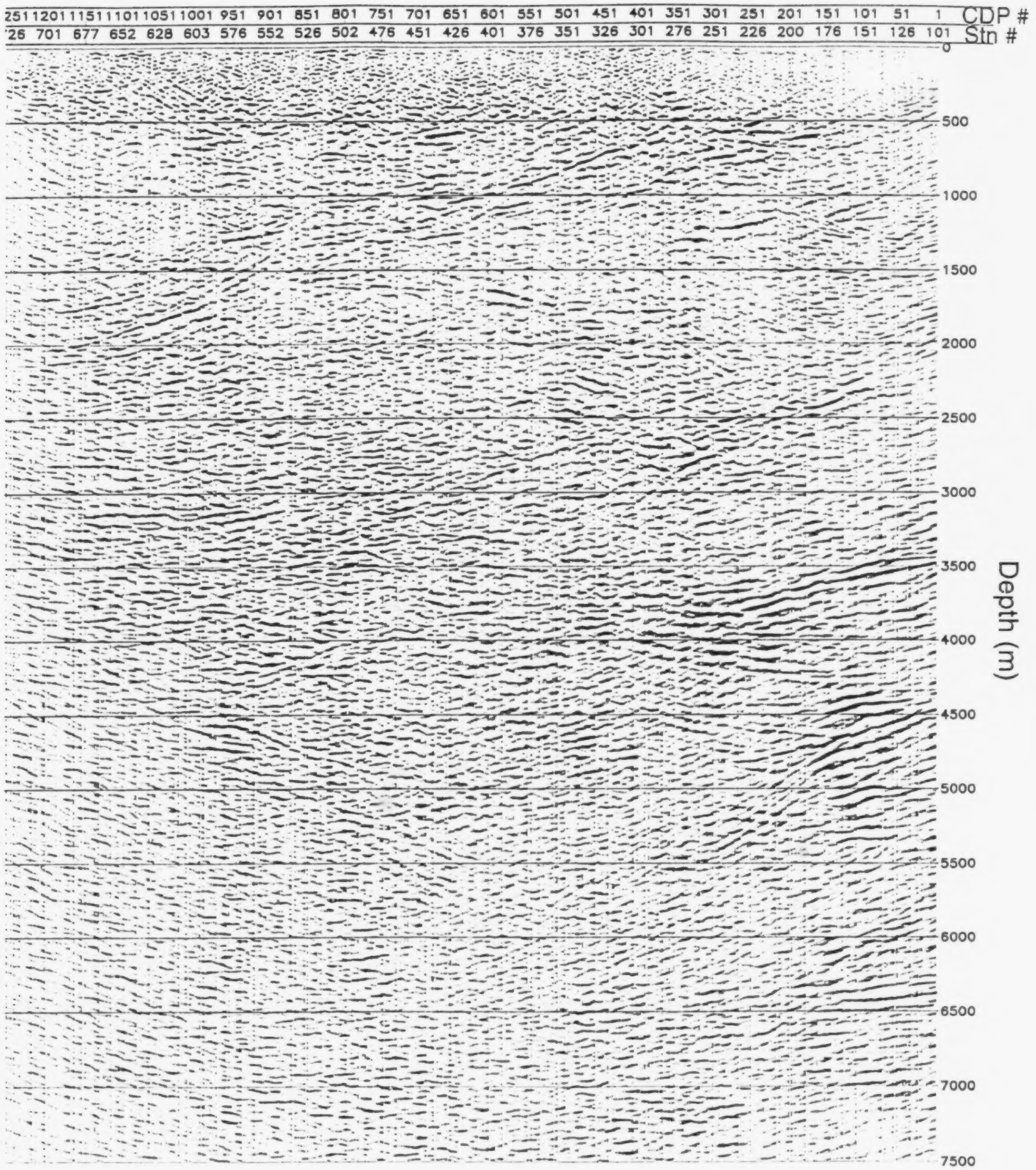

Figure 7. Kirchhoff depth migration for line HST98-001

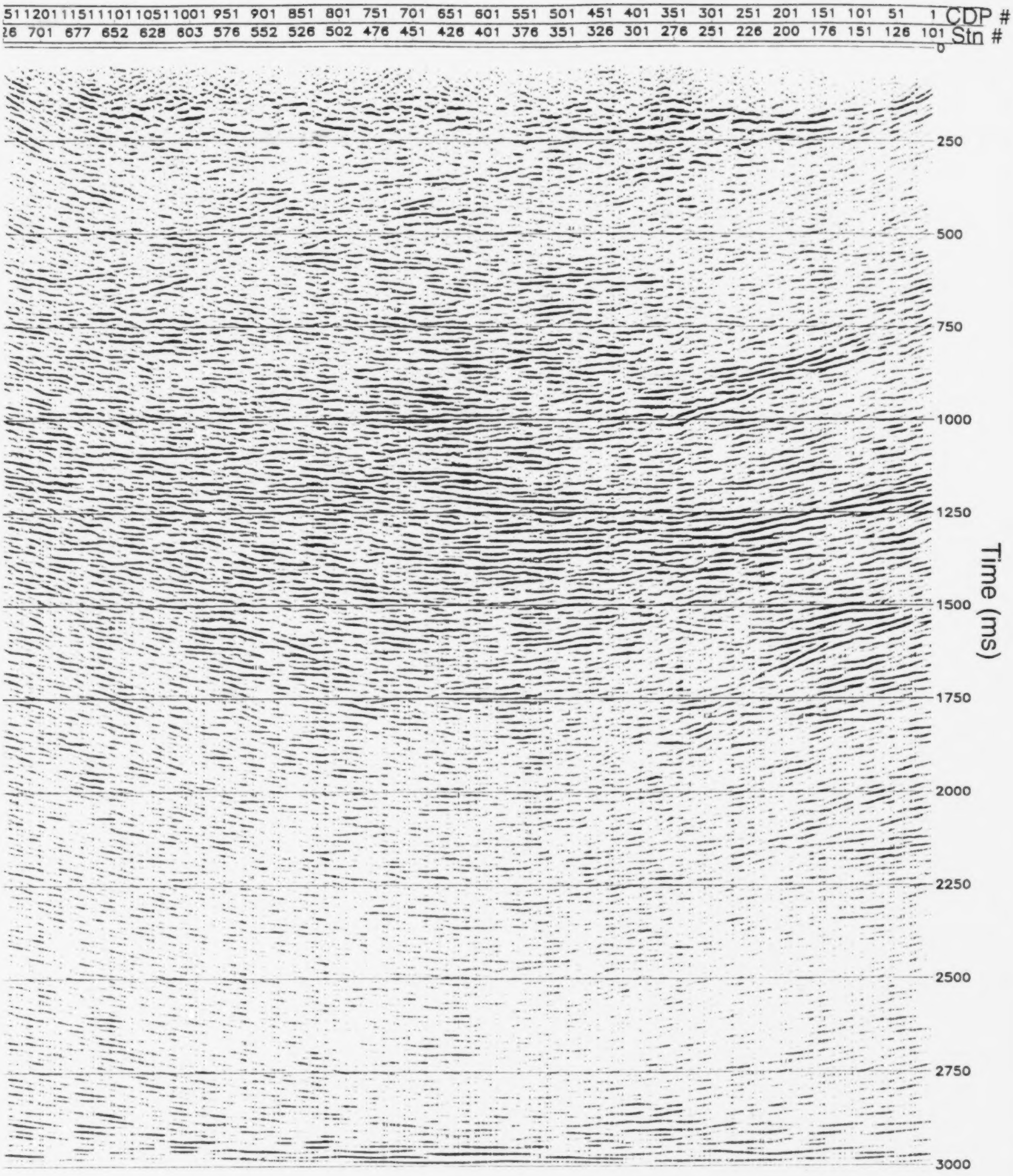

Figure 8. Stack using EOM prestack migration for line HST98-001

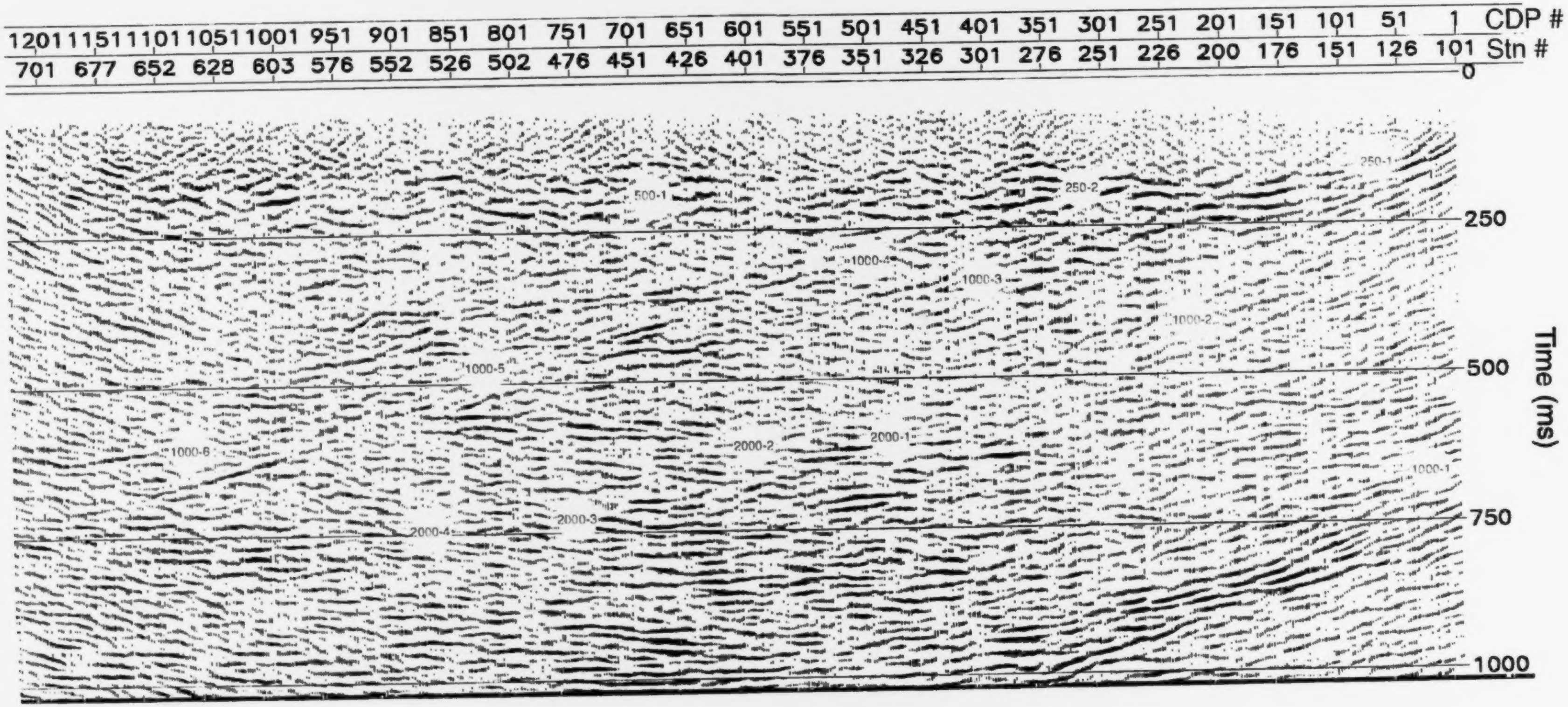

Figure 9. Top 1 s of the EOM migrated section for line HST98-001 with the locations of the scatterers found during the MUSIC stack analysis indicated. There is an example MUSIC stack for each of the anomalies indicated here in Appendix A. The number in the circles refer to the offset that was used for the scan and the anomaly number at that offset.

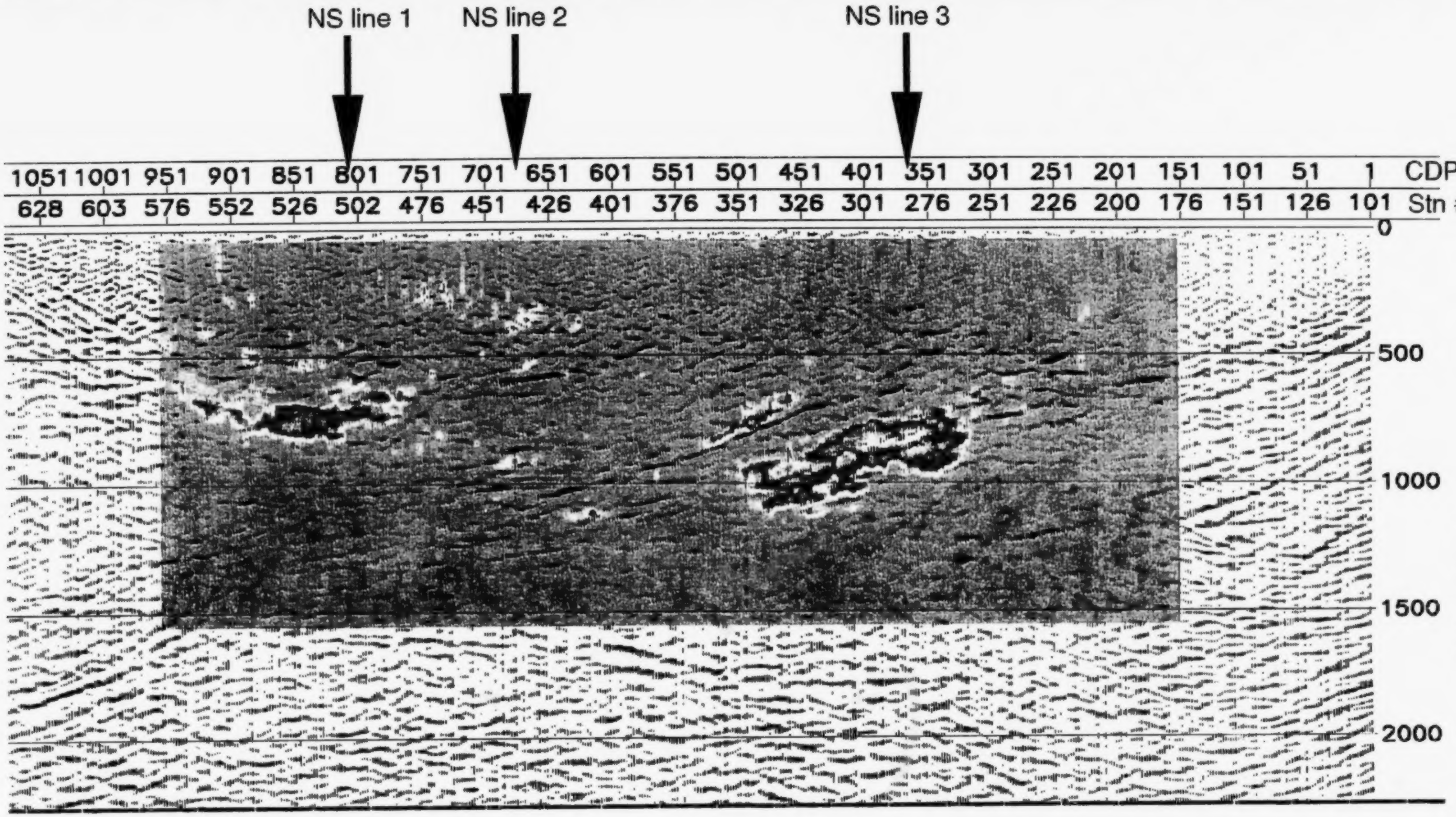

Figure 10. The top 2.5 km of the depth migrated section overlaying the results of the modified prestack Kirchhoff migration scattering analysis along the East-West line indicated on Figure 1. The colour map is normalized to the highest amplitude. Arrows indicate the location of North-South cross lines from the same scattering analysis (see Figure 11).

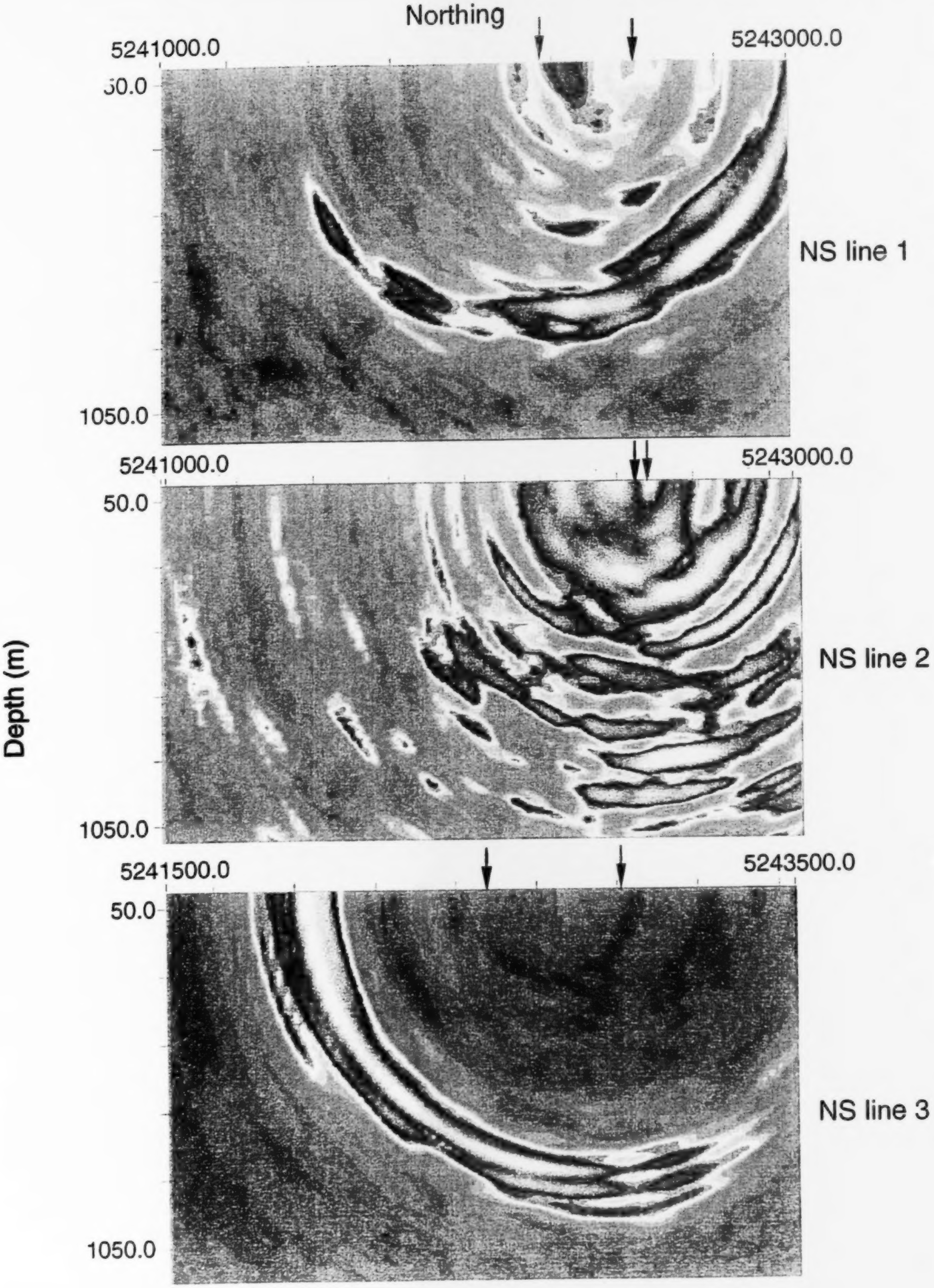

Figure 11. Three NS lines from the prestack Kirchhoff scattering analysis (see Figure 1 for locations). The black arrows indicate the position where the NS lines cross the EW line from Figure 10 and the blue arrows show the position that the NS lines cross the seismic line.

Appendix A: Music stacks at locations referred to on Figure 9.

Music stack, stn 127; 250-1 on Figure 9

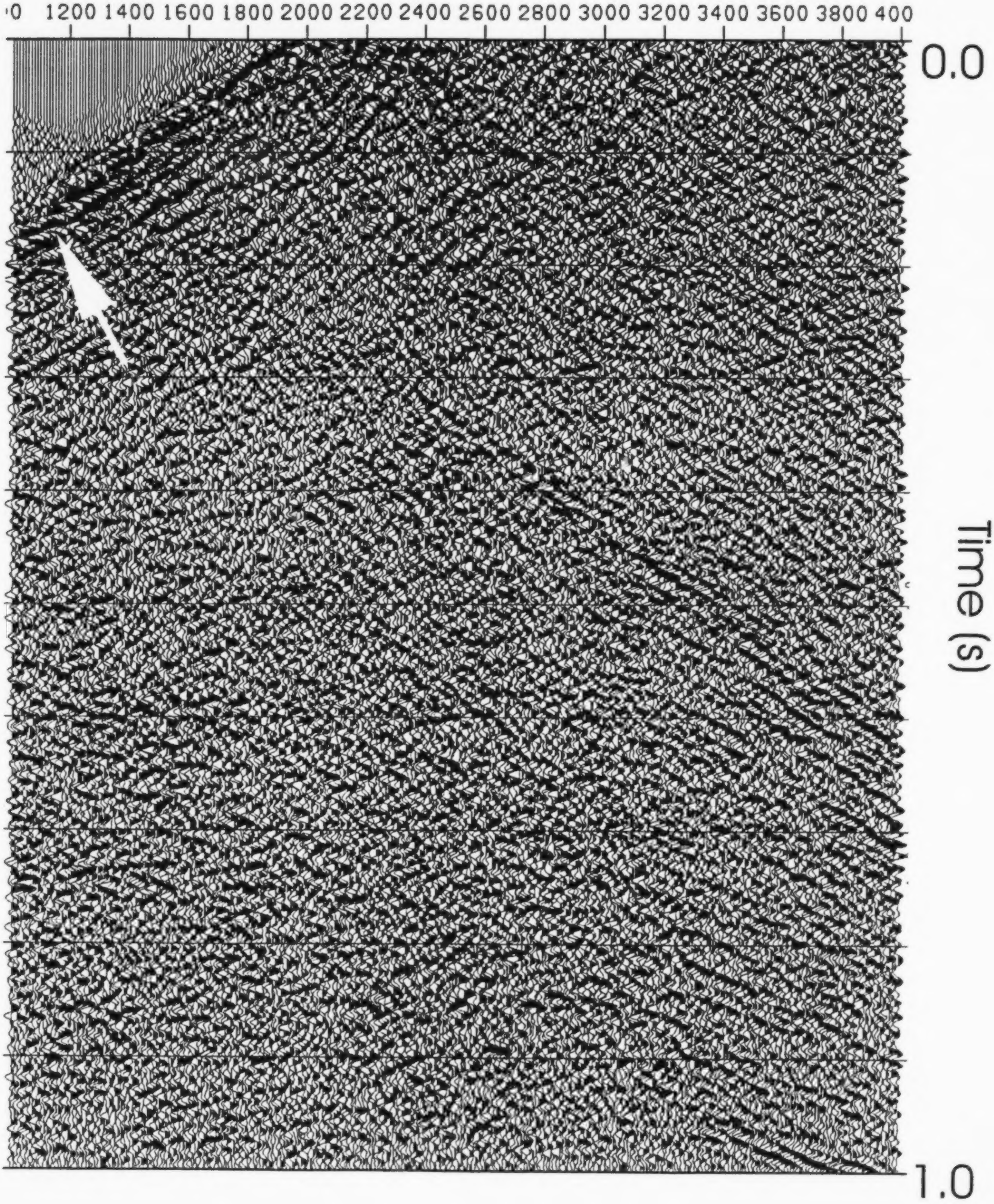

Music stack, stn 279; 250-2 on Figure 9

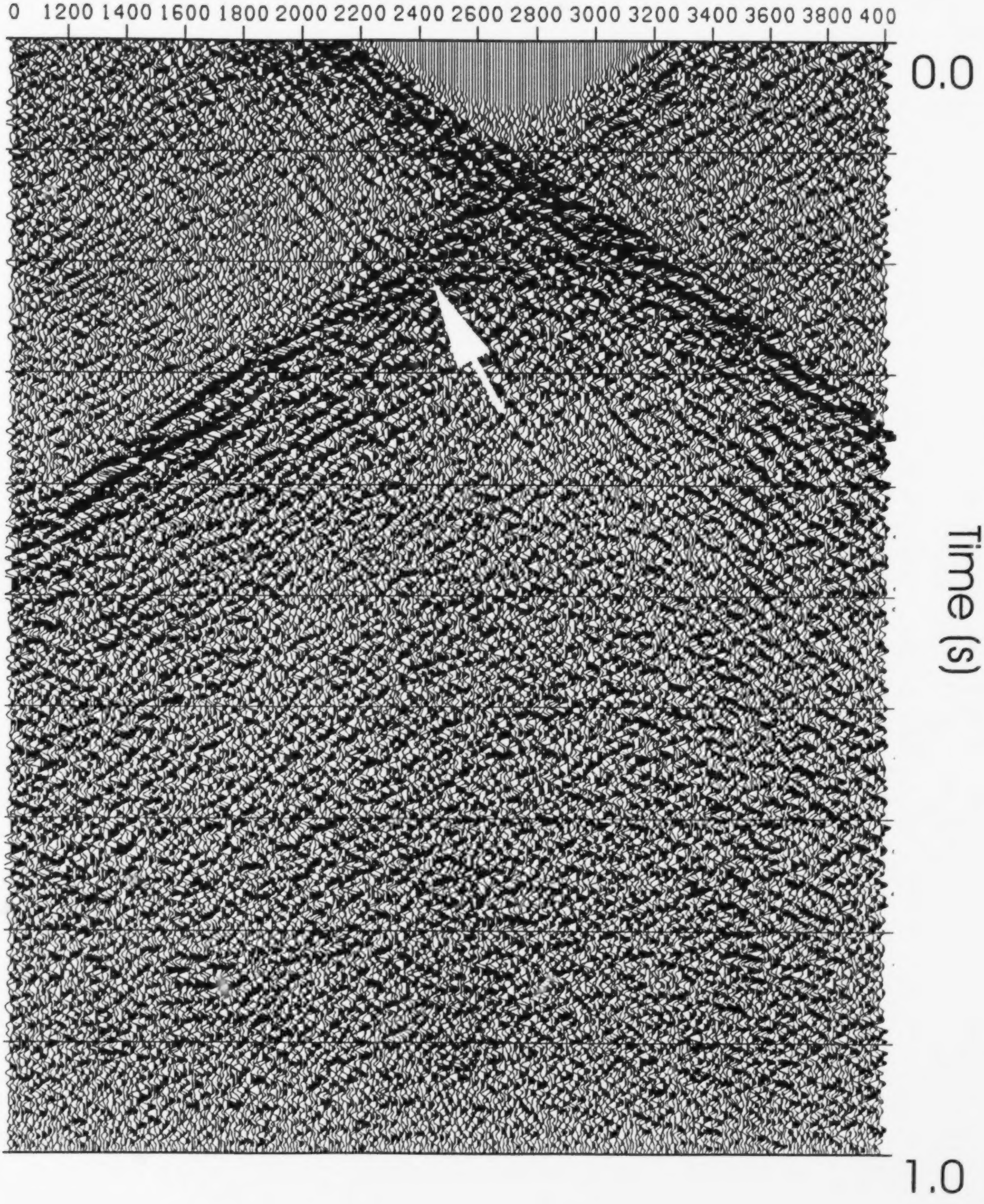

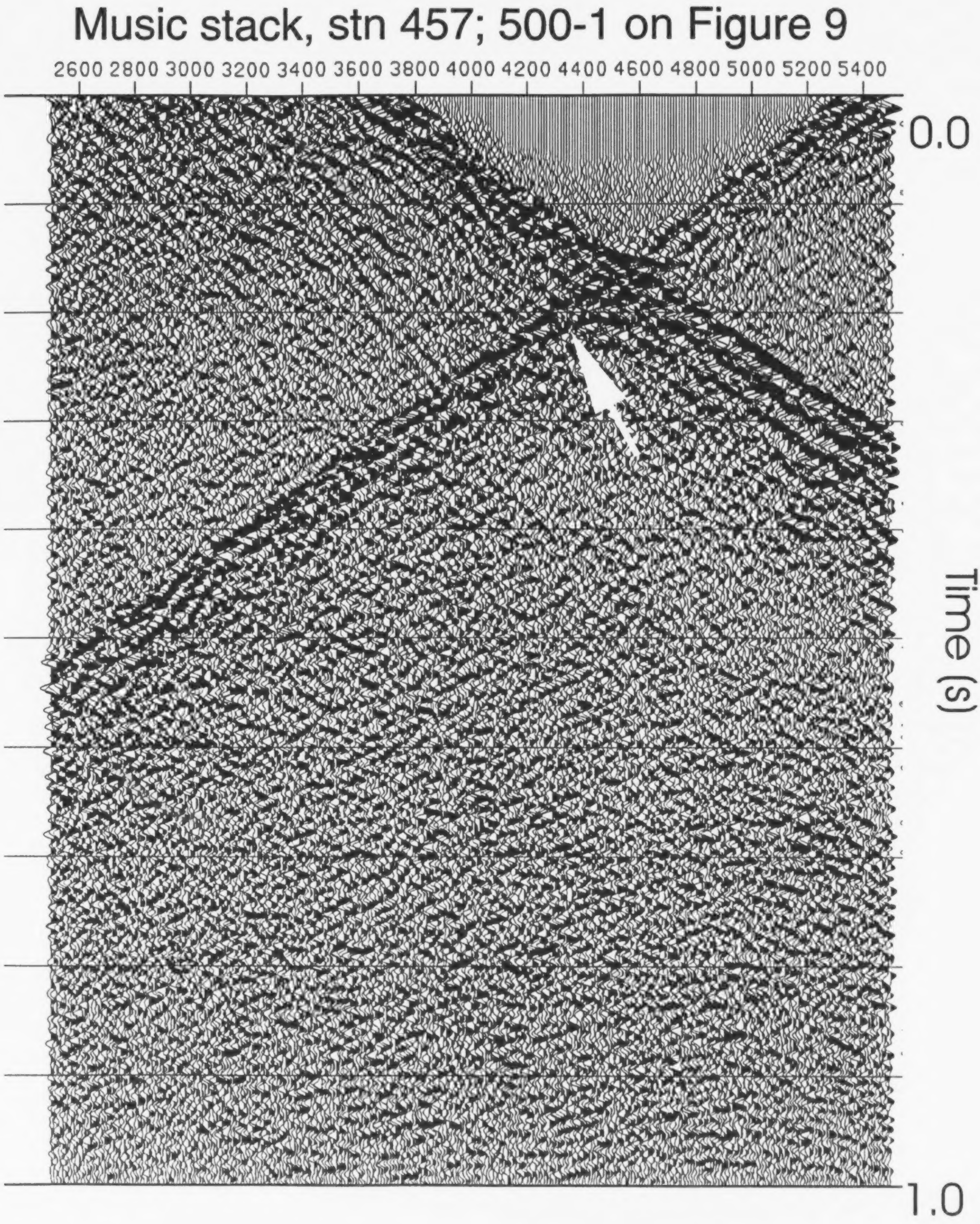

Music stack, stn 457; 500-1 on Figure 9

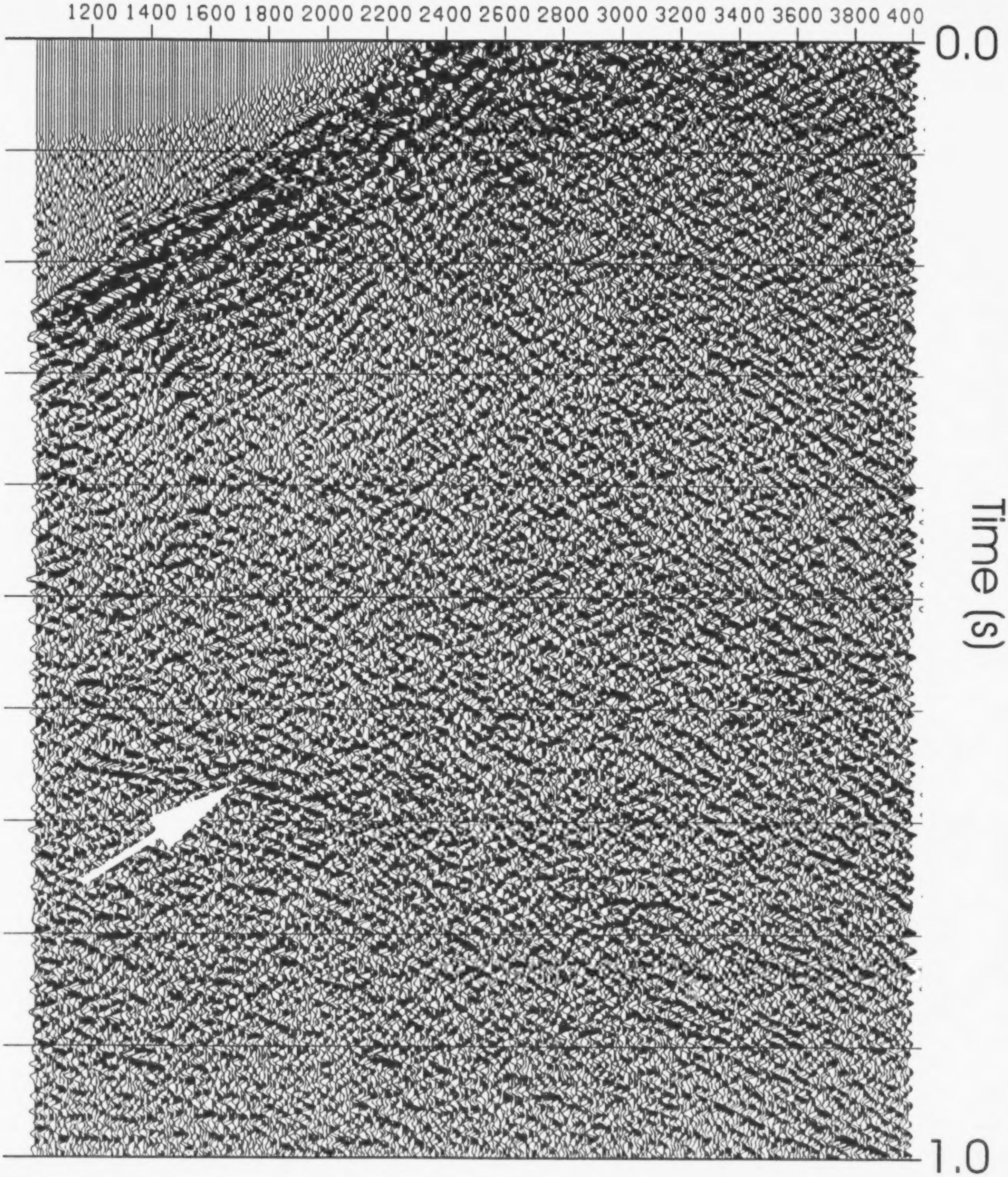

Music stack, stn 111; 1000-1 on Figure 9

Music stack, stn 211; 1000-2 on Figure 9

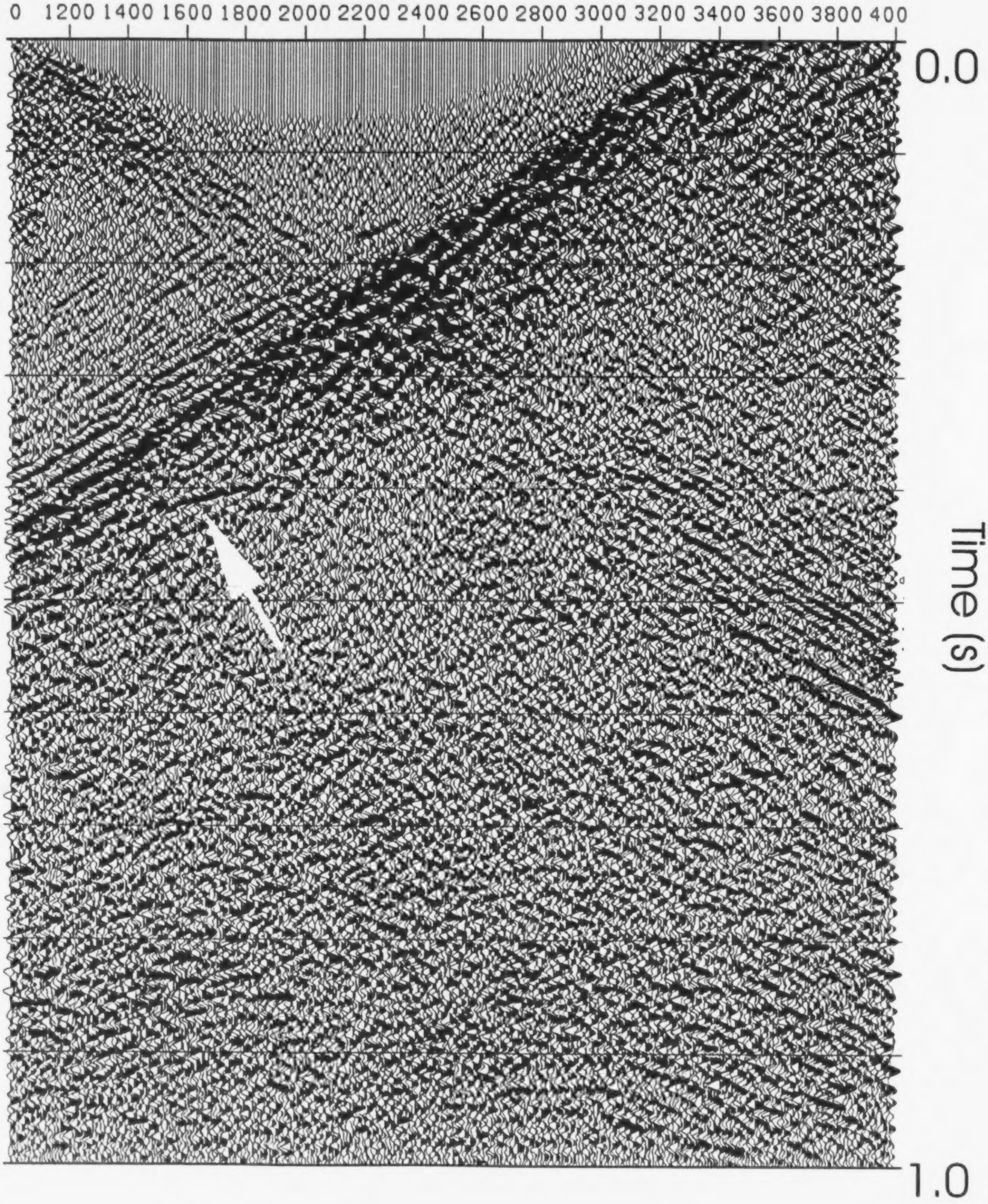

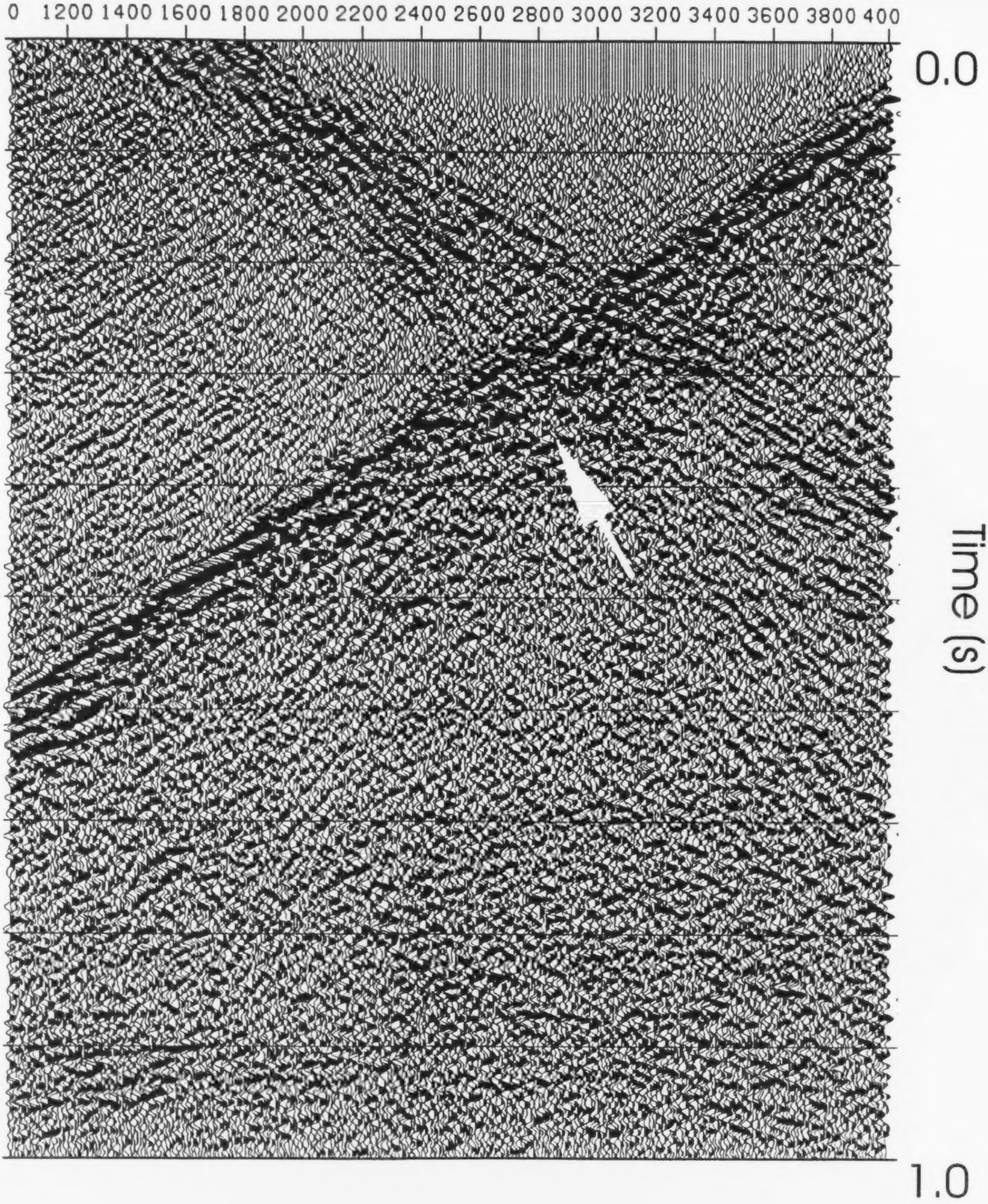

Music stack, stn 301; 1000-3 on Figure 9

Music stack, stn 337; 1000-4 on Figure 9

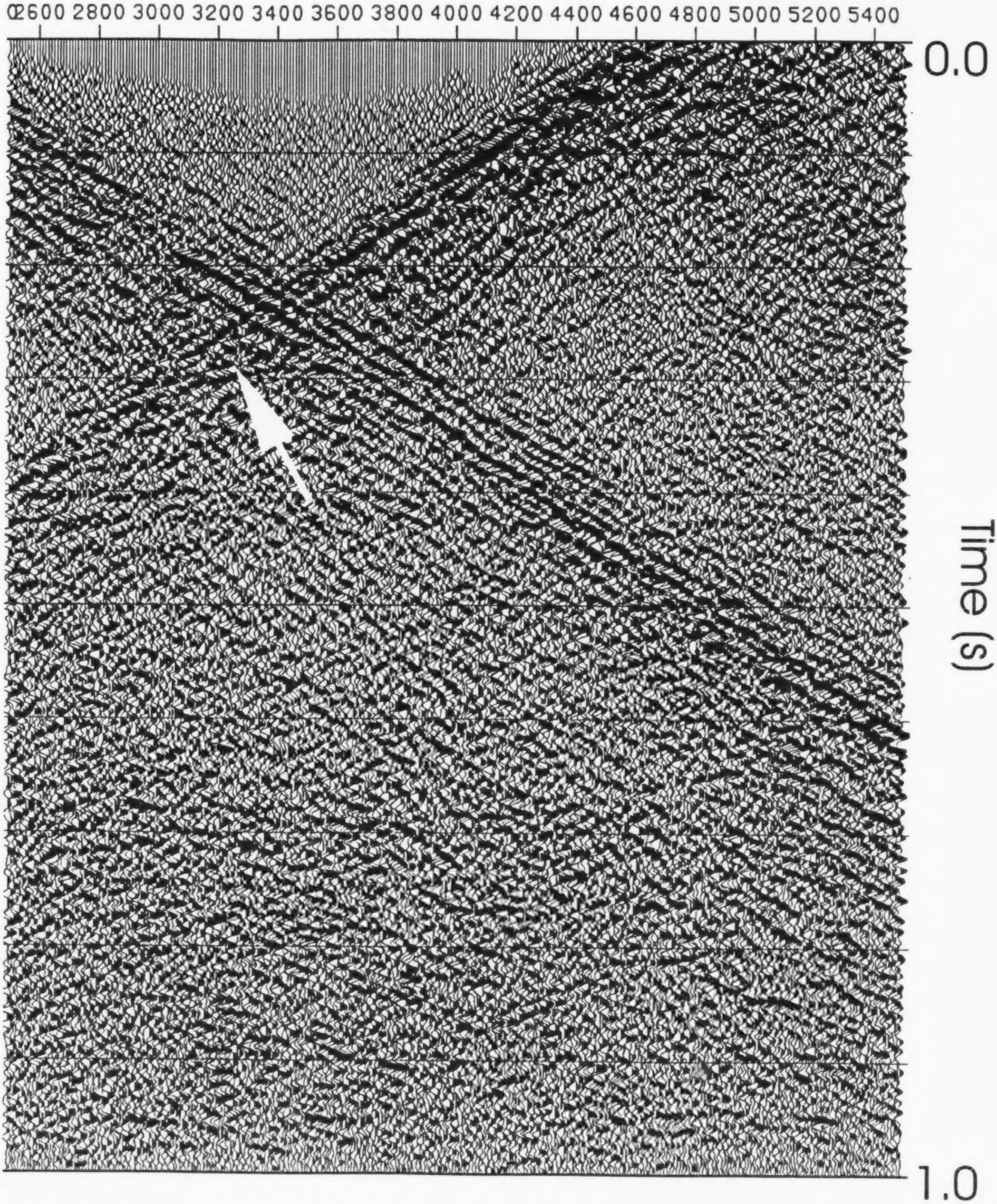

Music stack, stn 529; 1000-5 on Figure 9

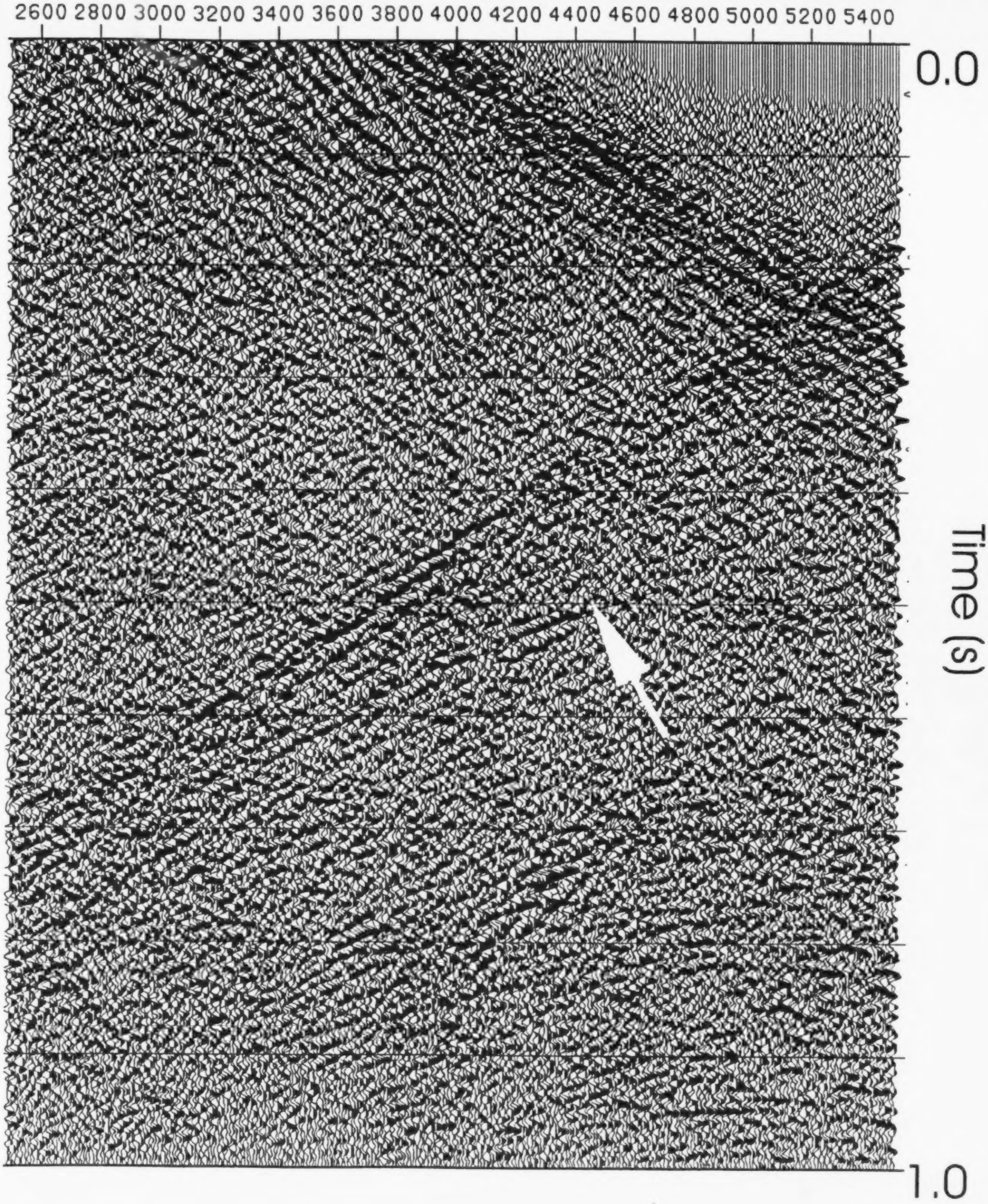

Music stack, stn 653; 1000-6 on Figure 9

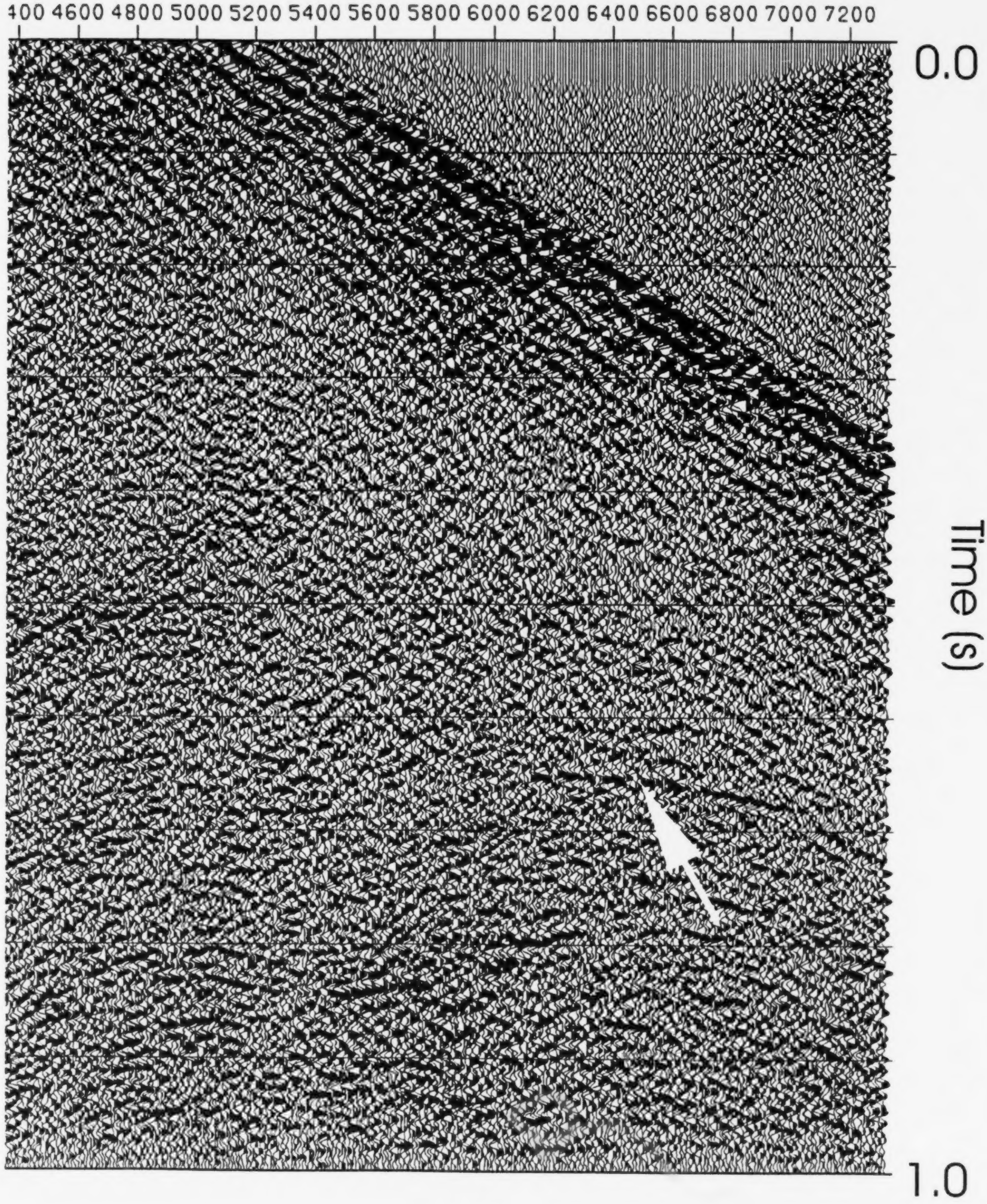

Music stack, stn 357; 2000-1 on Figure 9

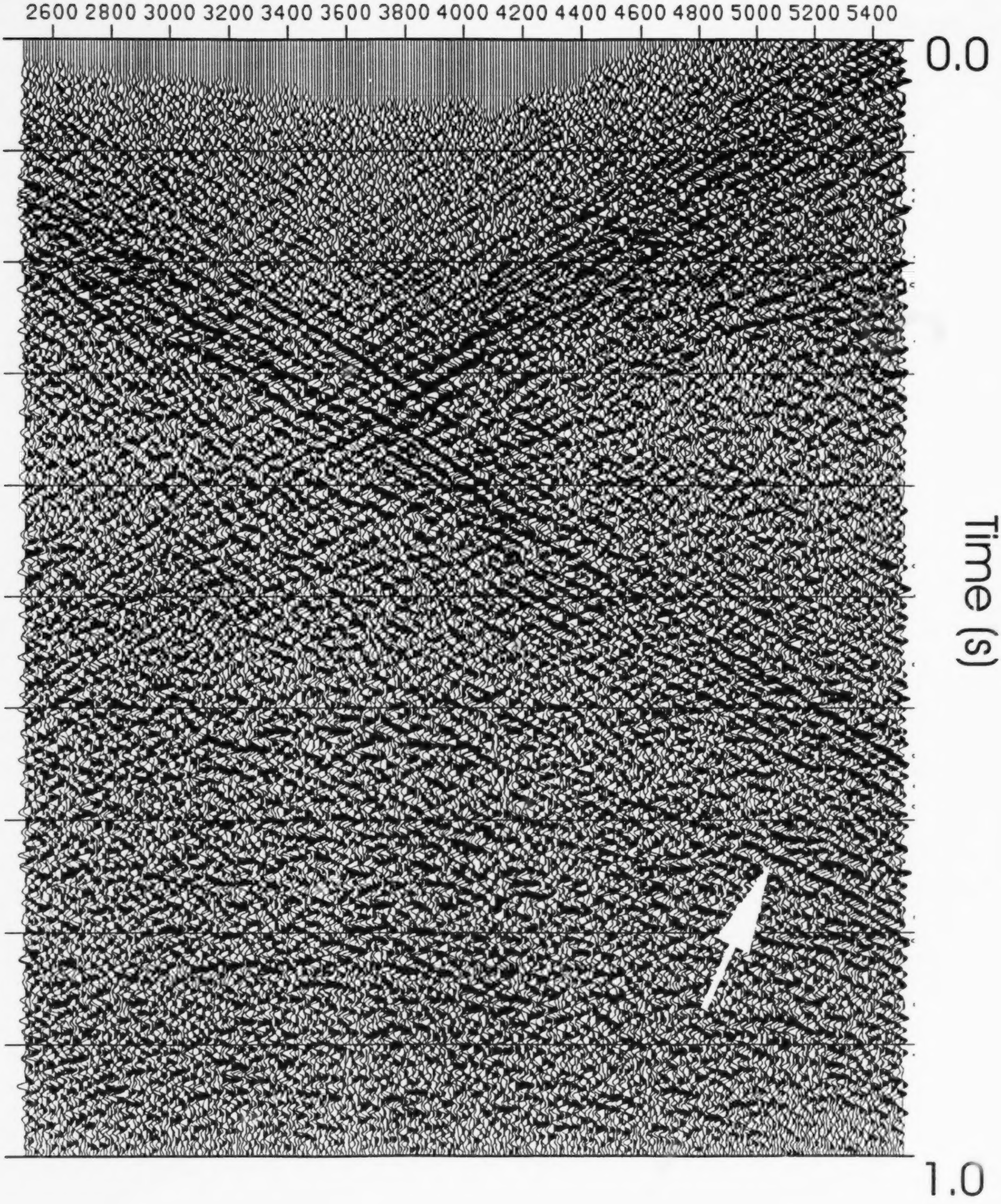

Music stack, stn 385; 2000-2 on Figure 9

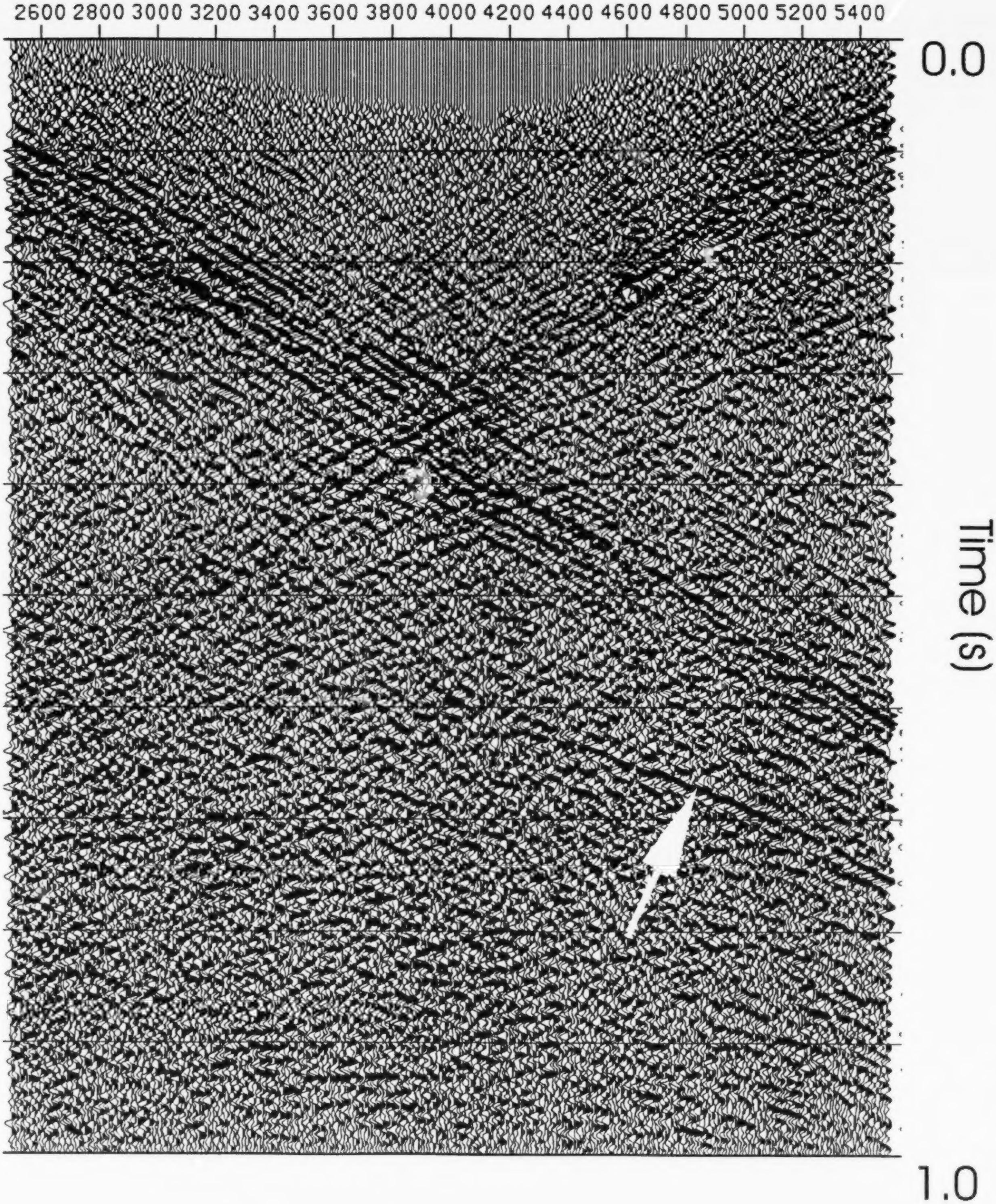

Music stack, stn 473; 2000-3 on Figure 9

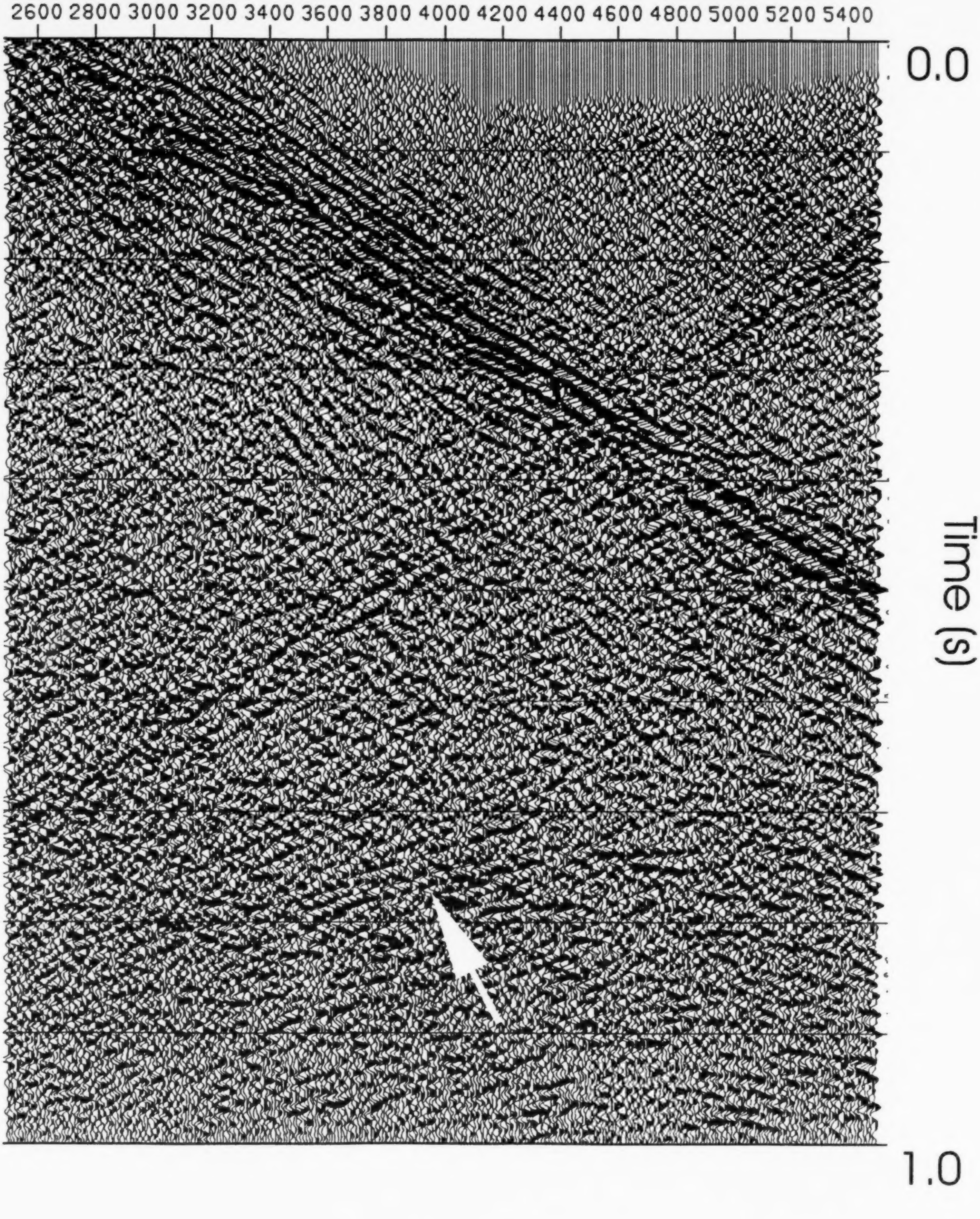

Music stack, stn 545; 2000-4 on Figure 9